

Human Embryonic Stem Cell-Derived Cardiomyocytes Migrate in Response to
Gradients of Fibronectin and Wnt5a: Implications for cardiac repair & congenital
heart defects

Kara N White Moyes

A dissertation
submitted in partial fulfillment of the
requirements for the degree of

Doctor of Philosophy

University of Washington
2013

Reading Committee:
Michael A Laflamme, Chair
Elaine W Raines
Dan Bowen-Pope

Program Authorized to Offer Degree:
Pathology

©Copyright 2013

Kara N White Moyes

University of Washington

Abstract

Human Embryonic Stem Cell-Derived Cardiomyocytes Migrate in Response to Gradients of Fibronectin and Wnt5a: Implications for cardiac repair & congenital heart defects

Kara N White Moyes

Chair of the Supervisory Committee:
Associate Professor Michael Laflamme
Department of Pathology

An improved understanding of the factors that regulate the migration of human embryonic stem cell-derived cardiomyocytes (hESC-CMs) would provide new insights into human heart development and suggest novel strategies to improve their electromechanical integration following intra-cardiac transplantation. Until now, nothing has been reported as to the factors controlling hESC-CM migration. Here we hypothesized that hESC-CMs would migrate in response to extracellular matrix and soluble signaling molecules previously implicated in heart morphogenesis. To test this, we screened candidate factors by transwell assay for effects on hESC-CM motility, followed by validation via live cell imaging and/or gap-closure assays. Fibronectin (FN) elicited a haptotactic response from hESC-CMs, with cells seeded on a steep FN gradient showing nearly five-fold greater migratory activity than cells on uniform FN. Studies with neutralizing antibodies indicated that adhesion and migration on FN are mediated by integrins α -5 and α -V. Next, we screened 10 soluble candidates by transwell assay and found that the non-canonical Wnt, Wnt5a, elicited a ~two-fold increase in migration over controls. This effect was confirmed using the gap closure assay, in which Wnt5a-treated hESC-CMs showed ~two-fold greater closure than untreated cells. Studies with

microfluidics-generated Wnt5a gradients showed that this factor was chemoattractive as well as chemokinetic, and Wnt5a-mediated responses were inhibited by the Frizzled-1/2 receptor antagonist, UM206. In summary, hESC-CMs show robust pro-migratory responses to FN and Wnt5a, findings that have implications for both cardiac development and cell based therapies.

Table of Contents

List of Figures.....	iii
List of Tables.....	iv
List of Abbreviations.....	v
Chapter 1: Human embryonic stem cell-derived cardiomyocytes:	
Derivation, Electrical Integration and Migration	1
1.1 hESCs for Heart Repair	1
1.1a Derivation and Culture of hESCs	2
1.1b Generation of Cardiomyocytes from hESCs.....	4
1.1c hESC-CMs Integrate & Restore Function to Damage Myocardium.....	7
1.1d Guided hESC-CM Migration to Improve Electromechanical Integration.....	8
1.2 Cardiomyocyte Migration During Heart Morphogenesis.....	9
1.2a Heart Tube Closure.....	10
1.2b Addition of Secondary Heart Field to the Heart Tube.....	11
1.2c Trabeculation of Ventricular Myocardium.....	12
1.2d Septation.....	13
1.3 Fibronectin and Integrins in Migration.....	19
1.3a Fibronectin Structure and Assembly.....	19
1.3b Integrins and Migration.....	20
1.3c Fibronectin Receptors Integrins $\alpha 5\beta 1$ and $\alpha V\beta 3$	21
1.3d Fibronectin in the Healing Infarct.....	21
1.4 Wnt5a Overview.....	23

1.4a Wnt Trafficking.....	23
1.4b Non-canonical Wnt signaling.....	24
1.4c Wnt5a Receptors.....	25
1.4d Wnt Signaling in Infarcted Myocardium.....	27
1.5 Thesis Overview.....	28
Chapter 2: hESC-CMs Migrate in Response to Gradients of Fibronectin & Wnt5a.....	37
2.1 Summary.....	37
2.2 Materials and Methods.....	38
2.3 Results.....	43
2.4 Conclusions.....	49
Chapter 3: Discussion.....	66
3.1 Limitations of this Study.....	66
3.2 Implications of this Work.....	67
3.2a hESC-CM Migration as a Model for Human Heart Morphogenesis.....	67
3.2b Guided Migration to Enhance Electrical Coupling.....	69
3.3 Future Studies.....	70
3.3a Is Wnt5a Pro-Migratory for Cardiomyocytes in the Developing OFT?.....	70
3.3b Elucidating the Mechanism of Wnt5a Mediated Migration.....	71
3.3c In Vitro Modeling of In Vivo Studies.....	71
Acknowledgements.....	75
References.....	77

Figures

Figure 1.1 Illustration of the valves and septal structures of the mature heart.....	30
Figure 1.2 Myocardialization of the OFT septum.....	31
Figure 1.3 Wnt5a signaling.....	32
Figure 2.1 hESC-CMs migrate spontaneously on two-dimensional surfaces.....	51
Figure 2.2 hESC-CMs exhibit a haptotactic response to fibronectin.....	53
Figure 2.3 hESC-CM migration on fibronectin is dependent on gradient slope.....	54
Figure 2.4 Wnt5a is a pro-migratory factor for hESC-CMs.....	55
Figure 2.5 Wnt5a is chemotactic for hESC-CMs.....	56
Figure S2.1 Generation and genetic selection of hESC-CMs.	57
Figure S2.2 Agarose diffusive printing generates surface-bound gradients of FN.....	58
Figure S2.3 Effect of Col VI on the haptotactic response to FN.....	59
Figure S2.4 Additional studies to characterize the migratory response to Wnt5a.....	60
Figure S2.5 Effect of Wnt5a on haptotactic response to FN.....	62
Figure 3.1 Methods for determining Wnt5a signaling mechanism(s).....	73
Figure 3.2 Wnt5a does not alter expression of MMPs in hESC-CMs.....	74

Tables

Table 1.1 Methods for differentiating cardiomyocytes from hESCs.....	33
Table 1.2 Timeline of morphogenetic events during heart development.....	34
Table 1.3 Non-canonical Wnt signaling is critical for outflow tract septation.....	35
Table 2.1 Candidate Pro-Migratory Molecules tested in Transwell Screen.....	63
Table 2.2 Human Integrin Primers.....	64
Table 2.3 Human Frizzled and other Wnt Receptor Primers.....	65

Abbreviations

AS - Atrial Septum
AVC - Atrioventricular Canal
AVS - Atrioventricular Septum
bFGF - basic Fibroblast Growth Factor
BMP4 - Bone Morphogenetic Protein 4
CHD - Congenital Heart Defect
CM -Conditioned Media
CMs - Cardiomyocytes
CNC - Cardiac Neural Crest
Col I - Collagen I
Col VI - Collagen VI
DM - Dorsal Mesocardium
DMP - Dorsal Mesenchymal Protrusion
DSCAM - Downs Syndrome Cell Adhesion Molecule
Dvl - Dishevelled
EB - Embryoid Body
ECG - Electrocardiogram
ECM - Extracellular Matrix
EMT - Epithelial to Mesenchymal Transition
FN - Fibronectin
Fzd - Frizzled
GCaMP3 - Calcium sensitive green fluorescent protein
GPCR – G-Protein Coupled Receptor
hESC-CMs - human Embryonic Stem Cell-Derived Cardiomyocytes
hESCs - human Embryonic Stem Cells
HGF - Hepatocyte Growth Factor
HH - Hamburger Hamilton developmental stage
Int - Integrin
IVS - Interventricular Septum
KDR - Kinase insert Domain Receptor (aka VEGF Receptor 2)
LN - Laminin
MC - Mesenchymal Cap
MCK - Muscle Creatine Kinase
MHC - Myosin Heavy Chain
MLC - Myosin Light Chain
NRG - Neuregulin
OFT - Outflow Tract
PCP - Planar Cell Polarity (non-canonical Wnt pathway)

PDGF - Platelet Derived Growth Factor
PKC - Protein Kinase C
PTA - Persistent Truncus Arteriosis
Ror2 - Receptor tyrosine kinase-like Orphan Receptor 2
RTK - Receptor Tyrosine Kinase
SDF1 α - Stromal Derived Factor 1 α
SHF - Secondary Heart Field
TGF β - Transforming Growth Factor β
T β 4 – Thymosin β 4
Vangl2 - Van Gogh-like 2
VEGF - Vascular Endothelial Growth Factor
VN – Vitronectin

Chapter 1: hESC-CMs: Derivation, Electrical Integration and Migration

Human embryonic stem cell-derived cardiomyocytes (hESC-CMs) are valuable as both a model for human heart development and as a potential cell source for restoring function to infarcted myocardium. The goal of this study is to identify factors that regulate hESC-CM migration in order to provide new insights into human heart morphogenesis and to develop novel strategies for improving their electromechanical integration following intra-cardiac transplantation. Until now [1], no one has described hESC-CM migration, so **we hypothesized that hESC-CMs would migrate in response to extracellular matrix and soluble factors that are important for heart morphogenesis.**

Below is a review of the derivation of hESC-CMs and the in vivo studies that demonstrate their ability to electrically integrate with host myocardium. I will then briefly describe a strategy that utilizes pro-migratory extracellular matrix and/or soluble factors to promote migration and improve electrical integration of hESC-CMs in scar tissue. Section 1.2 is an extensive survey of the development literature, detailing events in which cardiomyocytes migrate and the factors that are known, or speculated to drive their movement during these processes. Our screen of these candidate molecules (described in Chapter 2) revealed that fibronectin and Wnt5a are pro-migratory for hESC-CMs. To expand our understanding of these two proteins, I will end this chapter with a review of fibronectin, Wnt5a and their receptors, highlighting their roles in cellular migration and in the healing infarct.

1.1 Human Embryonic Stem Cell-Derived Cardiomyocytes for Heart Repair

Heart disease is the leading cause of death among Americans due in part to the heart's limited capacity to regenerate following ischemic injury. The tissue damaged during

myocardial infarct is eventually replaced with a non-contractile scar, resulting in decreased cardiac output. In recent years, cell based therapies have received considerable attention as a means to restore contractile function to lost myocardium. Human embryonic stem cells (hESCs) provide an attractive source of cardiomyocytes for this purpose because they are highly proliferative, capable of self-renewal and reliably differentiate into populations of high cardiac purity. Perhaps most important is the demonstrated ability of hESC-CMs to improve cardiac function when transplanted into damaged heart tissue [2-5]. Recently, our lab has shown that hESC-CMs are capable of electrically coupling with healthy host myocardium, suggesting that the improved contractility observed in injury models may be the result of mechanical force generated by injected cells [5]. However, this study also revealed that grafts in cryoinjured hearts often remain surrounded by insulating scar tissue and do not completely integrate with the host. This implies that by improving host-graft integration, perhaps via guided migration, it may be possible to achieve an even greater restoration of function to damaged hearts.

In this section I will review the derivation of hESCs, methods for generating cardiomyocytes from these pluripotent cells and the animal studies highlighted above. I will then propose a novel strategy to direct the migration of engrafted hESC-CMs toward the border zone, thereby increasing the likelihood of host-graft contact and electromechanical coupling.

1.1a Derivation and Culture of hESCs

In 1998, Thomson and colleagues built on their experience with non-human primate ESCs [6] to successfully derive human ESCs [7]. hESCs are derived from the inner cell mass of pre-implantation stage blastocysts that are obtained from donated human embryos generated for reproductive purposes. The pluripotency of hESCs was confirmed by their ability to form tri-

lineage embryoid bodies (EBs) in vitro and teratomas (benign tumors including tissues from all three embryonic germ layers) in immunodeficient mice [7]. Undifferentiated hESC cultures form compact colonies of cells with prominent nucleoli and a large nuclear-to-cytoplasmic ratio. They express high levels of alkaline phosphatase and transcription factors associated with self-renewal such as Oct4, Sox2, Nanog, and Rex1 [6, 8, 9]. hESCs also express high levels of telomerase [6, 10], a ribonucleic acid-protein complex that adds hexameric repeats to the telomeres at the ends of chromosomal DNA to compensate for the loss that occurs during replication.

Like their murine counterparts, undifferentiated hESCs were originally maintained by direct growth on a monolayer of irradiated mouse embryonic fibroblasts, cells that support proliferation and self-renewal. Unfortunately, this method had two major limitations: 1. the feeder cells had to be eliminated from the culture before transplantation and 2. exposure to non-human cells raised concerns about xenopathogens. Because of these limitations, hESCs are now commonly grown in media conditioned by either mouse embryonic fibroblasts [11] or human feeder alternatives [12-14]. Ideally, feeders and feeder-conditioned medium would be replaced with recombinant or synthetic factors to facilitate the scaled production of hESCs for cell therapies. With this goal in mind, multiple investigators have developed methods for long-term culture of hESCs in chemically-defined media [15-18]. Most of these protocols include high levels of basic fibroblast growth factor (bFGF), a molecule that is critical for hESC self-renewal [18-21]. Ongoing small-molecule screens [22-24] and proteomic analyses of feeder-conditioned media [25, 26] will likely lead to more efficient methods for hESC culture.

1.1b Generation of Cardiomyocytes from hESCs

Many investigators have obtained cardiomyocytes from pluripotent stem cells by forming EBs in the presence of high concentrations of fetal calf serum (a method first pioneered by Doetschman and colleagues with murine ESCs) [27, 28]. Unfortunately, the cardiac purity of these cell preparations is typically very low. Less than 10% of human EBs show beating activity [29], and <1% of the total differentiated cell population is cardiac [3, 30, 31]. The purity of these preparations can be improved by mechanically dissecting spontaneously beating areas (to ~30-70% cardiomyocytes [2, 29]), but this tedious method is not scalable to clinical applications (it is estimated that more than one billion cardiomyocytes are lost in a human infarct [32]). Motivated by this need for reproducible, scalable protocols that yield high purity preparations of cardiomyocytes, investigators have applied knowledge from developmental biology to direct the differentiation of hESCs to cardiomyocytes. Some examples of the advancements made over the last 10 years are highlighted below and summarized in **Table 1.1**.

Endoderm Co-culture. The Mummery group was one of the first to apply knowledge from embryology to guide the differentiation of hESCs to cardiomyocytes. Their approach involves the co-culture of hESCs with END-2 cells, (a visceral endoderm-like derivative of P19 cells [33]), in an attempt to recapitulate the cardio-inductive effects of anterior endoderm [34-36]. This method yields approximately one cardiomyocyte per 20 starting undifferentiated hESC [37]. Interestingly, culture with END-2 conditioned medium gave similar results, indicating that soluble factors were responsible for cardiogenesis. The efficacy of the END-2 conditioned medium was improved by insulin omission [38] and/or the addition of a small molecule inhibitor of p38 MAP kinase [39].

Activin A & BMP-4. Our group has also reported a protocol that uses defined factors to guide the differentiation of hESCs into cardiomyocytes. This protocol involves two members of the transforming growth factor- β (TGF β) superfamily that are known to exert time-dependent effects during cardiogenesis, activin A and bone morphogenetic protein-4 (BMP-4) [3]. Activin signaling promotes the induction of mesendoderm in the epiblast of model organisms [40-42] and ESC cultures [43-47]. Slightly later in development, the anterior endoderm and nearby ectodermal tissues release BMP-2 and BMP-4, inducing cardiogenesis in the pre-cardiac mesoderm [48, 49]. In an attempt to recapitulate this sequence of signaling events, we serially treat monolayers of hESCs with activin A and BMP-4 in serum-free medium. The growth factors are removed on day 5 following induction, and the cells are maintained in serum-free medium for an additional 2-3 weeks. This method typically yields preparations that are 30-60% cTnT positive [3, 50].

Interestingly, the inductive capacity of activin A is suppressed by insulin/phosphatidylinositol 3-kinase signaling [51]. This likely relates to the previously discussed anti-cardiogenic effects of insulin on cells differentiated in the presence of END-2 conditioned medium [38]. Consistent with these observations, the Palecek group has recently shown that omission of insulin from a similar activin/BMP-4 protocol greatly increases the efficiency of cardiomyocyte differentiation [52]. However, the anti-cardiogenic effect of insulin can be rescued by stage specific inhibition of canonical Wnt signaling [52]. (This protocol, which manipulates Wnt signaling in completely defined, growth factor-free conditions, is described in more detail below).

Wnt inhibition in KDR+ progenitors. In the developing embryo, canonical Wnt signaling is required for induction of early mesoderm, but it inhibits the induction of pre-cardiac

mesoderm at later time points [53, 54]. The Keller group has developed a protocol that takes advantage of this biphasic effect of Wnt while manipulating the TGF β family signaling as above. They first generate a primitive streak-like population by treating EBs with BMP-4, bFGF, and activin A for 4 days [55]. They then dissociate the EBs, sort out KDR⁺ multi-potent progenitor cells and seed them in a monolayer. These cells are then treated with Dkk1 to prevent the inhibitory actions of Wnt signaling on cardiogenesis, VEGF to promote expansion of the KDR⁺ population, and bFGF to support the growth of the cardiovascular lineages. This protocol reportedly generates populations of ~40-50% cardiomyocytes [56].

Matrix sandwich method. The Kamp group has developed a protocol that starts by sandwiching hESCs in matrigel, a commercially available extracellular matrix (ECM) [57]. The rationale is to promote the epithelial to mesenchymal transition that epiblast cells undergo during gastrulation to eventually give rise to pre-cardiac mesoderm. This ECM sandwich generates N-cadherin-positive mesenchymal cells that are then treated with serial application of Activin A, bone morphogenetic protein 4, and basic fibroblast growth factor. This protocol generates hESC-CMs with high purity (up to 98%) and yields up to 11 cardiomyocytes for every input pluripotent cell [57].

Modulation of Wnt/ β -catenin with small molecules. Most recently the Palecek group has reported a differentiation protocol that, like the Keller lab protocol, takes advantage of the biphasic effects of Wnt signaling, but does not require cell sorting and is growth factor free [58]. Briefly, Wnt signaling is promoted in a monolayer of hESCs with the Glycogen Synthase Kinase 3 (GSK3) inhibitor, CHIR99021, and subsequently inhibited by a small molecule inhibitor of porcupine that prevents the Wnt ligand from being produced. This method typically

yields populations that are 80-98% cardiac after 14 days of differentiation and has proven effective over several cell lines[58].

1.1c hESC-CMs Integrate & Restore Function to Damaged Myocardium

Regardless of how they are derived, hESC-CMs have structural, electrical, mechanical and calcium handling properties of definitive, albeit immature cardiomyocytes and are able to proliferate in vitro and in vivo [31, 59-61]. They express sarcomeric proteins including α -actinin, cardiac troponins I and T, α - and β -myosin heavy chains (MHCs), atrial- and ventricular- myosin light chains (MLC2v and MLC2a), desmin, and tropomyosin [29, 33, 62-65] and exhibit spontaneous contractile activity. hESC-CMs express gap junction proteins [33, 61, 62, 66] and exhibit intercellular electrical communication in vitro and in vivo [67-71].

These properties make hESC-CMs an attractive cell source for cardiac repair, and indeed they have been shown to improve cardiac function when transplanted into infarcted mouse and rat hearts [2-4]. Until recently, electromechanical integration had not been directly demonstrated in injured hearts, so it was unclear if hESC-CMs were improving contractile function by direct addition of new force-generating units or by other “paracrine” effects. Previous studies had shown that hESC-CMs are capable of electrically integrating with the host when injected into healthy heart tissue [68, 69, 71] or if graft-host contact is made through the use of infarct-spanning engineered tissue constructs [72, 73]. To ask whether hESC-CMs injected into scar tissue can electromechanically couple with the host, Shiba & Fernandes et al transplanted hESC-CMs that expressed GCaMP3 (a green fluorescent calcium sensing protein that increases in intensity in the presence of high intracellular calcium) into intact and cryoinjured guinea pig hearts[5]. They then used intra-vital fluorescence imaging to correlate the GCaMP3 signal with

the host ECG. Consistent with the findings mentioned above, grafts in uninjured hearts demonstrated 1:1 host-graft coupling in all cases. However, grafts in injured hearts contained both coupled and uncoupled regions, a reflection of the heterogeneity of contact between islands of graft within the insulating scar and the bordering myocardium. In spite of this incomplete coupling, injection of hESC-CMs into injured hearts attenuated the deterioration of fractional shortening seen in vehicle or non-CM controls 28 days after injection [5].

1.1d Guided hESC-CM Migration to Improve Electromechanical Integration

The study above provides the first proof of concept that engrafted hESC-CMs have the potential to restore mechanical function to damaged myocardium by providing synchronously contracting, force generating units. Because injected cells were not always fully integrated, we speculate that enhancing the integration of the graft cells would result in an even greater restoration of contractile function. One approach to increasing host-graft contact would be to chemically attract hESC-CMs from sites of injection toward intact myocardium. A chemotactic gradient could be established by delivering slow-release microspheres loaded with a pro-migratory growth factor into healthy border tissue. A similar strategy has been explored with the goal of promoting angiogenesis in infarcted heart tissue by delivering bFGF in gelatin microspheres [74, 75]. In one study, delivery of microspheres with a transendocardial injection catheter resulted in a retention rate of 15% in healthy pig hearts and 19% in a 1-week old infarct [74].

Alternatively (or perhaps simultaneously) one could stimulate random migration by injecting hESC-CMs in a delivery vehicle that contains a pro-migratory ECM molecule. While many injectable scaffolds including fibrin, alginate and chitosan [76], are being investigated for

repair and vascularization of the infarcted area, ours is the first study to consider the migratory properties of cardiomyocytes. This is at least in part due to the fact that factors that drive their migration have not yet been described. We hypothesized that hESC-CMs would migrate in response to extracellular matrix and soluble signaling molecules important for heart morphogenesis and that once identified, these factors could be used therapeutically as described above. In the next section I will review what is known about cardiomyocyte motility in the context of cardiac development and identify candidate pro-migratory factors for hESC-CMs.

1.2 Cardiomyocyte Migration During Heart Morphogenesis

Just as investigators have taken clues from embryology to define signals that would direct the differentiation of epiblast-like hESCs into cardiomyocytes, we can turn to cardiac development to identify potential drivers of hESC-CM migration. Here I will review the events that take early cardiomyocytes from their site of specification to their home in the chambered heart and will discuss factors that are known, or speculated to play a role in migration in these processes.

It is important to note that the major motivation here is to identify pro-migratory factors for hESC-CMs that will ultimately be used to help regenerate damaged adult myocardium. However, knowledge gained in this study can also be used to expand our understanding of human heart development. hESC-CMs provide a unique opportunity to ask questions about cardiomyocyte biology that cannot be answered in the human fetal system. For this reason I will pay particular attention to examples of congenital heart defects that could possibly be explained by aberrant cardiomyocyte migration. **Table 1.2** provides a timeline of events, from heart tube

closure to outflow tract (OFT) septation, for human, mouse and chick and highlights potential pro-migratory molecules in each process.

1.2a Heart tube closure

The heart is the first organ to function during vertebrate development, forming from bilaterally symmetric cardiogenic fields that migrate and fuse at the embryonic midline to create a contractile heart tube [77]. In the chick, these bilateral heart fields form at HH 7 and 8 when the lateral plate mesoderm on either side of the midline splits into two layers to create somatic (dorsal) and splanchnic (ventral) mesoderm [78]. (Note: in mammals, a single cardiogenic field takes the shape of a “crescent” that is continuous across the midline). The pre-cardiomyocytes now residing in the splanchnic mesoderm, undergo mesenchymal to epithelial transition, expressing N-cadherin at the apical surface of what will become myocardial epithelium [79]. These cardiogenic fields migrate to the ventral embryonic midline and by HH stage 8-9 begin to express sarcomeric myosin and cardiac troponin I [80]. By stage 10 the fields have fused and the newly formed heart tube begins beating [81].

What drives the migration of these cardiogenic fields to the midline? The bilateral fields move ventro-medially as the adjacent pharyngeal endoderm folds to form the foregut. If pharyngeal endoderm is ablated, the fields fail to migrate to the midline and instead form two hearts, a condition known as *cardia bifida* [82]. (Incidentally, this observation revealed that each of the cardiogenic fields possesses the program to form a functioning, chambered heart and that cardiogenesis does not rely on tube fusion). Early experiments by Lash attempting to identify an endodermally-derived chemotactic factor for cardiogenic mesoderm were unsuccessful [83]. Lash did however demonstrate that fibronectin is laid down at the mesoderm-endoderm

interface in a gradient that coincides with the direction of cell movement [84] suggesting that fibronectin acts as a haptotactic guide for pre-cardiac mesoderm. Subsequent studies in the mouse [85] and zebrafish [86] have confirmed the importance of fibronectin in the formation of the primary heart tube. In zebrafish lacking fibronectin, cardiac myosin light chain 2 positive cells do not fuse at the midline, rather they move in a disorganized manner resulting in the formation of two bilateral hearts [86]. In this model, adherens junctions between the myocardial precursors do not form properly, suggesting that cell-fibronectin interactions are important for epithelial organization and that this epithelial integrity is required for the migration of the myocardial progenitors.

1.2b Addition of secondary heart field to the heart tube

Next, the heart tube undergoes rightward looping while cells from the secondary heart field (SHF) are added to lengthen the inflow (venous) and outflow (arterial) ends of the tube. The SHF contributes cells to the cardiac outflow tract, right ventricle and a major part of atrial myocardium, while the linear heart tube gives rise predominantly to the left ventricle [87, 88]. At the time of heart tube closure, cardiac progenitor cells of the SHF are situated in splanchnic mesoderm medial to the primary cardiogenic fields (reviewed in [89]). As the heart tube forms, the progenitors maintain this position, continue to proliferate and delay differentiation.

At HH 14 the progenitors begin to express HNK1, a marker of translocation, and migrate into the outflow tract [90]. As these cells move nearer the lengthening heart tube, they begin to express sarcomeric myosin [90] suggesting that signals from the OFT induce their differentiation. This process is necessary for the arterial pole of the lengthened tube to properly align with the ventricles after looping and if perturbed results in early embryonic lethality [78,

89]. In humans, malformations of the of the arterial pole due to misalignment contribute to many congenital heart defects including tetralogy of Fallot, double outlet right ventricle and overriding aorta [78]. Despite this, no chemotactic or haptotactic factors have been identified for these migrating cardiac progenitors. FGF8 signaling is essential for the process, though it likely is necessary for proliferation and differentiation rather than migration [88]. Sonic hedgehog (Shh) is also required for normal arterial pole formation and proliferation of SHF progenitors [91]. Interestingly, blocking of Shh with cyclopamine has a modest inhibitory effect on migration of explanted SHF cells prior to their differentiation to cardiomyocytes [91], but there is no evidence for a pro-migratory effect of Shh on progenitors in ovo.

1.2c Trabeculation of Ventricular Myocardium

The looping heart tube then next begins to balloon and trabeculate, forming the presumptive ventricles. Trabeculae are projections of myocardium extending from the compact outer wall into the cardiac jelly, the ECM between the myocardial and endothelial layers. This spongy, contractile tissue adds surface area to the compact layer, which is not yet vascularized and relies on diffusion of oxygen and nutrients from inside the tube [92].

It is well established that signaling from the endocardium to the ventricular myocardium initiates proliferation, differentiation, and migration of cells out of the compact layer and into the lumen of the ventricle [92-94]. NRG1 from the endocardium dimerizes ErbB2 and ErbB4 receptors on myocardial cells, inducing them to proliferate and populate the emerging trabeculae [95]. NRG1 signaling can also activate focal adhesion kinase [96], a key requirement for cell motility, suggesting a role for NRG1-mediated cardiomyocyte migration in the trabeculation process. Consistent with this, a recent study in zebrafish demonstrated that ErbB2

was required not only for cardiomyocyte proliferation, but also for delamination and migration of these cells into the trabecular protrusions [94]. The non-canonical Wnt, Wnt11 [97], and the membrane spanning receptor/ligand Semaphorin 6D [98], are also necessary for spatial organization of cardiomyocytes and compact layer expansion, though their precise role in cardiomyocyte migration is unknown.

1.2d Septation

Septation of the atrial and ventricular chambers, the atrioventricular canal (AVC) and the OFT is necessary for forming a four-chamber heart from the primitive heart tube. Abnormal development of the septal structures accounts for the majority of all congenital heart defects (CHD) which occur in ~1% of newborns and account for 20% of spontaneous abortions and 10% of stillbirths [99-102]. Therefore, an understanding of the various cell populations and complex morphogenetic events that contribute to creating a four-chambered heart is of clinical importance.

The looped heart tube is segmented into the atrium, ventricle, the atrioventricular canal (AVC, the junction between atria and ventricles), and the OFT and is composed of an inner endocardial lining and an outer myocardial layer. Septation begins when local tissue swellings, termed endocardial cushions, are formed in the lumen of the AVC and proximal portion of the OFT by an accumulation of extracellular matrix (cardiac jelly) between the endocardial and myocardial layers [103]. Meanwhile, a muscular interventricular septum (IVS) emerges within the ventricular chamber and grows superiorly to fuse with these AV cushions, dividing the chamber into left and right ventricles [104]. The IVS also connects with OFT cushions to separate the ventricle into systemic and pulmonary outlets. At this time, another muscular

septum, the primary atrial septum, grows from the atrial roof towards the AVC [103]. This muscular outgrowth partially septates the atrial chamber leaving a temporary opening (the ostium primum) that allows blood to enter the left atrium from the right atrium to bypass the pulmonary circulation. Each of these morphogenetic events is described in more detail below with particular attention given to the cell types and signaling molecules involved. **Figure 1.1** provides a guide of the important structures and cellular origins. Where appropriate, I will discuss how perturbations in cardiomyocyte migration during these processes might lead to CHD.

Atrial Septum. Separation of the atria occurs as two septation events. First, the primary muscular septum grows toward the AVC from the atrial roof, carrying with it a mesenchymal cap on its leading edge [104]. This muscular outgrowth partially separates the atrial chambers, leaving an opening (the ostium primum) between the mesenchymal cap and the AV cushions. At the same time, a mesenchymal mass termed the dorsal mesenchymal protrusion (DMP) migrates from the SHF dorsal to the heart tube, and bulges into the atrial chamber [105]. The DMP, mesenchymal cap and AV cushions then merge to seal the ostium primum [103]. The mesenchymal cap and DMP are later “muscularized” to form a myocardial septum, but the AV cushions remain mesenchymal [104]. While the ostium primum is closing, the upper end of the primary atrial septum breaks down, creating a second opening (the ostium secundum) between the right and left atria. Next, a second muscular septum is formed when part of the atrial roof folds inward. The primary and secondary atrial septum fuse postnatally to seal the second opening, completing the septation of atrial chambers [104].

Defects in the atrial septum are characterized as either primum or secundum depending on which ostia fails to close [78]. Ostium primum defects can occur when the primary septum

does not fuse with the AV cushions or DMP [106]. These are typically classified as AV defects, which are discussed below. Ostium secundum defects result from a septum primum that is of insufficient size to cover the entire opening, or from a septum secundum that fails to fully form[106].

To date, no chemotactic or haptotactic factors have been found responsible for the outgrowth of the primary septum or the inward folding of the secondary septum from the atrial roof. However, investigators have attempted to define a cardiomyocyte specific role in aberrant septation. In an effort to recapitulate the septal defects seen in trisomy 21 patients, Grossman et al created a mouse model that overexpresses collagen VI (Col VI) and the Down's Syndrome Cell Adhesion Molecule (DSCAM) under the cardiomyocyte specific, alpha MHC promoter. Genes for this extracellular matrix protein and adhesion receptor lie on chromosome 21 and have been implicated in heart defects associated with Down's Syndrome [107, 108]. They found that mice overexpressing these two proteins had atrial septal defects and that cardiomyocytes overexpressing DSCAM adhered more firmly to Col VI than wild type cells [109]. Interestingly, other septal defects typically associated with Down's Syndrome patients (AVD, VSD) were not seen in these animals, a possible reflection of the cardiac muscle specific promoter. The mechanism and classification (primum versus secundum) of the atrial defect are unknown, but these findings open the possibility that appropriate expression of these two molecules is important for cardiomyocyte migration out of the atrial roof to form a muscular septum.

Atrioventricular Septum. Four mesenchymal tissues are required for AVC septation: the mesenchymal cap of the primary atrial septum, the superior and inferior AV cushions, and the dorsal mesenchymal protrusion (a SHF derivative that protrudes into the dorsal aspect of the

atrial cavity) [103]. AV cushion mesenchyme is derived through epithelial-to-mesenchymal transformation (EMT) of endocardial cells that trans-differentiate, migrate into the cardiac jelly and proliferate to cellularize the cushions [103]. (Note: unlike the cushions of the OFT (discussed below), AV cushions do not muscularize in mammals [104]). The mesenchymal cap, which envelops the growing edge of a muscular atrial septum, also arises from the endocardium. These four tissues fuse at the AV canal, dividing it into mitral and tricuspid orifices that form the ventricular inlets.

Recent work showing that perturbations in DMP formation are responsible for many non-cushion AV defects (reviewed in [106]) has caused an increased interest in how this structure is developed. For example, trisomy 16 models of Down's Syndrome lack a DMP while other contributions from the SHF are intact [105]. This leads one to ask how the DMP arises from the dorsal mesocardium in the SHF, protrudes into the atrial chamber, and differentiates into muscle tissue. To answer these questions Goodeeris et al tested the hypothesis that hedgehog signaling was responsible for migration and differentiation. Interestingly, they found a decrease in migration of explanted dorsal mesocardium upon treatment with cyclopamine [110], suggesting that hedgehog is pro-migratory for this tissue. Additionally, in *Mef2c-AHF-cre; Smoflox/-* mutants, (a mouse in which the gene for Smoothed, the Shh receptor, is deleted from SHF cells), they found an ectopic population of MF20+ cells within the dorsal mesocardium, but no DMP [110]. Under normal circumstances, the DMP is muscularized via mesenchymal to myocardial transition after it enters the atrial chamber and fuses with the AVC [105]. This observation suggests that septation is not a pre-requisite for differentiation and that hedgehog signaling is necessary for appropriate migration and/or differentiation. One hypothesis is that hedgehog signaling is required to maintain a mesenchymal phenotype, and in

its absence, these progenitor cells differentiate to cardiomyocytes and fail to leave the dorsal mesocardium. Alternatively, Shh could act as a driver of DMP migration and in its absence cells fail to migrate and differentiate ectopically. In either case, it appears that Shh signaling in cardiomyocytes is not required for DMP formation, as there are no atrial septal defects in TnT-Cre; Smoflox/- mutants [110].

Interventricular septum. Within the ventricular chamber, an interventricular muscular septum emerges and grows superiorly to fuse with AV and OFT cushions, dividing the left and right ventricles and the ventricular outlets [104]. The muscular ventricular septum forms as the trabecular components at the apex of the developing left and right ventricles from the primary heart tube balloon inward [104]. There are no examples of aberrant cell migration leading to failure of the IVS to form. In fact, most ventricular septal defects are actually sub-aortic and are the result of failed septation of the proximal portion of the outflow tract (described below) [78].

Outflow tract septum. In order to completely separate pulmonary from systemic circulation, the outflow end of the tube must also divide into the right and left ventricular outlets that lead to the pulmonary artery and aorta. First, cardiac neural crest (CNC) and endocardial cells undergoing epithelial to mesenchymal transition (EMT) invade the cardiac jelly to form the proximal and distal OFT cushions (reviewed in [103, 111]). Eventual fusion of the distal cushions divides the OFT into aorta and pulmonary trunk. Failure of this process results in a single vessel arising from the ventricles, a defect termed persistent truncus arteriosus (PTA). Fusion of the proximal cushions septates the OFT into left and right ventricular outlets and fusion of this newly formed mesenchymal septum with the muscular IVS closes the interventricular foramen [104]. The aortic and pulmonic valves later develop at the junction of the proximal and distal regions of the OFT [103].

Unlike the AV cushions, the proximal OFT cushions later muscularize to form a myocardial sub-aortic septum. In this process, cells of the initially mesenchymal septum undergo apoptosis and are replaced by invading cardiomyocytes from the adjacent myocardial layer of the OFT [111] (**Figure 1.2**). Failure of the proximal cushions to myocardialize or fuse with the IVS, results in a sub-aortic ventricular septal defect [112-114]. Early experiments demonstrated that a myocardialization-inducing factor is likely produced by the non-myocardial portion of the OFT [115], but that factor has yet to be identified.

Many recent studies have revealed the importance of non-canonical Wnt signaling in this process. Wnts are a conserved family of secreted proteins that signal through the seven membrane spanning Frizzled receptors. In contrast to the canonical Wnt pathway which signals through β -catenin, non-canonical Wnt signaling includes the calcium and planar cell polarity (PCP) pathways and is responsible for cellular processes such as migration, invasion and polarity (described in more detail in section 1.4). Knockout of Ror2 [116-118], Fzd2 [119], Dishevelleds 2 or 3 [120], (all described receptors and downstream effectors of non-canonical Wnts), result in impaired OFT septation. In addition, when Vangl2, a component of the Wnt/planar cell polarity pathway, is deleted, cardiomyocytes fail to extend lamellipodia into the cushion mesenchyme to muscularize the OFT septum [113]. The importance of lamellipodia formation for proper OFT septation was further demonstrated in mice in which focal adhesion kinase (FAK) was conditionally inactivated in Nkx2.5 expressing cells. Lack of FAK, a key regulator of adhesion dynamics and a downstream target of Wnt5a [121], resulted in misalignment of the OFT with the ventricles and a failure to muscularize the outflow septum[114]. Additionally, chemotaxis toward serum was significantly impaired in isolated FAK-null cardiomyocytes [114].

Wnt11 and Wnt5a are two well studied non-canonical Wnts that are required for proper OFT septation [116, 122, 123] and have been implicated in the myocardialization process [99]. Wnt11 message is expressed at E10.5 and E12.5 by the outflow tract myocardium and myocardializing cardiomyocytes [113, 124] suggesting that while it might be necessary for successful septation [123], it is not acting as the non-myocardial guidance cue previously described [115]. Conversely, at these time points Wnt5a is expressed by cells of the cushion mesenchyme [113, 124], placing it at an appropriate location to guide the migration of cardiomyocytes into the adjacent cushion. Furthermore, Frizzled 2, a Wnt5a receptor, is expressed in the proximal OFT at E13 and is also required for proper septation [119]. Taken together, the above observations indicate a pathway whereby aberrant non-canonical Wnt5a signaling contributes to OFT defects by hindering the ability of cardiomyocytes to myocardialize the OFT cushions. (Summarized in **Figure 1.2** and **Table 1.3**). In spite of this mounting evidence, Wnt5a-mediated chemotaxis had not yet been described in cardiomyocytes prior to this study.

1.3. Fibronectin and Integrins in Migration

1.3a Fibronectin Structure and Assembly

The extracellular matrix (ECM) glycoprotein fibronectin (FN) is secreted as an approximately 440kD dimer, of two nearly identical monomers linked by a pair of disulfide bonds at their C-terminals [125]. Each monomer consists of an array of type I, II and III domains composed of two anti-parallel β -sheets. While the type I and II domains are stabilized by intra-chain disulfide bonds, type III domains do not contain any disulfide bonds, allowing them to partially unfold under applied force [126].

FN plays a critical role in a variety of morphogenetic processes including embryonic development and wound healing. In order for it to mediate these processes, FN must first be assembled into a functional fibrillar matrix that binds multiple ECM components and provides structural support for cell adhesion and migration [126]. FN exists in two forms: plasma (pFN) and cellular FN (cFN). pFN is secreted by hepatocytes into the blood where it remains in a non-fibrillar, soluble, form until it is assembled by activated platelets [127]. In contrast, cFN is assembled into an insoluble, functional matrix as it is secreted by the cell. $\alpha 5 \beta 1$ integrin receptors on the cell surface bind the RGD motif located in the 10th type-III domain of the soluble dimer [126]. The cells stretch and partially unfold fibronectin, unmasking cryptic sites that allow other fibronectin molecules nearby to associate and bind [128]. These fibronectin-fibronectin complexes branch and stabilize into an insoluble fibrillar matrix.

1.3b Integrins and Migration

Cell migration is characterized by a cycle of membrane protrusion and matrix adhesion at the leading edge followed by release of adhesions at the cell's rear. Protrusions are formed when the actin cytoskeleton polymerizes and pushes the cell membrane forward. Integrins are membrane spanning hetero-dimeric receptors that mediate migration by connecting the actin cytoskeleton to the underlying ECM. For optimized cell speed and directional persistence, integrin-ECM adhesions must assemble and disassemble in a polarized manner [129].

Cell polarity can be cell-intrinsic or can arise from the extracellular environment. Gradients of haptotactic (surface bound) or chemotactic (soluble) stimuli, such as FN or Wnt5a, can promote the asymmetric activation of evenly distributed receptors. Downstream of these activated receptors and upstream of integrins, Rho GTPases regulate actin polymerization and

adhesion dynamics [129] to polarize the cell and generate a protrusion toward the highest concentration of stimulus [130]. Importantly, chemoattractive molecules can also induce polarization and migration even when presented homogeneously [130]. This phenomenon, termed chemokinesis, reflects the cell's intrinsic ability to self-polarize.

1.3c Integrins $\alpha 5\beta 1$ and $\alpha V\beta 3$

Eleven integrin heterodimers are reported to interact with fibronectin [126], but integrins $\alpha 5\beta 1$ and $\alpha V\beta 3$ are the ones that are most commonly described as mediating migration and adhesion. While $\alpha 5\beta 1$ is considered of major importance for FN assembly, loss of $\alpha 5$ in cells and mice revealed that FN can also be assembled by integrin αV [131-133].

While the two integrin dimers have some overlapping functions, they are not identical in their abilities. Danen et al demonstrated that expression of $\alpha 5\beta 1$ promoted a contractile, fibroblastic morphology with centripetal orientation of cell-matrix adhesions, high RhoA activity and random migration [134]. In contrast, cells expressing $\alpha V\beta 3$ displayed adhesions distributed across the ventral surface, low RhoA activity and highly persistent migration at a rate similar to that of the $\alpha 5\beta 1$ expressers [134]. The exact reason for the different actions of the two integrin dimers is not yet known, but the observation might be explained by the requirement of $\alpha 5$ to interact with a second site in addition to RGD to obtain maximum binding affinity [135]. This second site termed the "synergy region" is located in the ninth type III module adjacent to the RGD motif and contains the PHSRN minimal sequence [126].

1.3d Fibronectin in the Healing Infarct

In the adult heart, FN expression is relatively low but is greatly increased in response to

injury [136]. Under normal conditions cFN is secreted into the extracellular space where it is associated with the basal lamina to which cardiomyocytes adhere [137]. Following a myocardial infarction however, various isoforms of FN can be found regulating inflammation, fibroblast differentiation and angiogenesis in order to heal the damaged tissue [127, 138]. The process of wound healing comprises a series of events that eventually replaces damaged myocardium with scar tissue. This process can be divided into three phases characterized by acute inflammation (1 hour-4 days), proliferation (4-14 days) and maturation of scar tissue (14 days-2 months) [138]. The details of these events and the roles of FN are described below.

Following a myocardial infarct, the initial death of cardiomyocytes triggers up-regulation of chemokines, cytokines (IL-1 β , IL-6, IL-8, TNF- α) and adhesion molecules (ICAM-1, E-selectin) that initiate the inflammatory phase of the healing response [139]. During this phase, activated matrix metalloproteinases (MMPs) degrade the existing cardiac ECM and process cytokines and chemokines, altering their activity [139]. The hyperpermeable vasculature allows for extravasation of FN and fibrinogen, leading to formation of a plasma-derived provisional matrix. Infiltrating leukocytes use this matrix as a scaffold and remove dead cardiomyocytes from the infarct region [138].

Once the debris is cleared, anti-inflammatory cytokines such as IL-10 and TGF- β initiate the transition to the proliferative phase [139]. In this phase the provisional matrix is degraded and cFN is secreted by fibroblasts, macrophages and endothelial cells [127, 138]. Fibroblasts proliferate and differentiate into contractile cells, termed myofibroblasts, a process that is driven in part by binding of integrin α 4 β 7 to ED-A FN (a splice variant of FN with an extra domain "A") [127, 138, 140]. Myofibroblasts help to contract the wound and deposit a collagen-based matrix that supports the structure and morphology of the cardiac tissue. This matrix is deposited

first in the border zone and then in the center of the infarct, filling in the spaces left void by dead cardiomyocytes [138]. Another important event that occurs during the proliferation phase is the formation of a rich capillary network that reperfuses the injured site with blood. Within this newly vascularized tissue FN isoforms possessing the alternatively spliced ED-A and ED-B domains are highly up-regulated around neovessels and capillary sprouts where they act as an important cue to regulate angiogenesis [127]. In the final stage of wound healing most fibroblasts and vascular cells undergo apoptosis and the matrix is cross-linked to form a dense acellular collagen-based scar [138].

Above I have shown that in addition to being a matrix for cellular adhesion, FN acts as a conduit for infiltrating inflammatory cells, a differentiation signal for fibroblasts and a guidance cue during angiogenesis. The various responses to FN are dictated by its isoform (e.g. plasma, cellular, ED-A, ED-B) and the integrin expression profile of exposed cells. In Chapter 2 I show that hESC-CM adhesion and migration on FN depends on integrins $\alpha 5$ and αV . This information suggests that in order to create the desired pro-migratory environment for engrafted hESC-CMs while avoiding off target effects of FN on other cells, it may be best to inject hESC-CMs in a hydrogel that contains the RGD motif (the ligand for $\alpha 5$ and αV) rather than the full-length molecule.

1.4. Wnt5a Overview

1.4a Wnt trafficking

Wnts are a family of secreted, lipid-modified glycoproteins that regulate processes such as cellular differentiation, migration and tissue patterning. They act as morphogens by diffusing from their source to form a concentration gradient in the surrounding tissue and distant cells

translate this signal into spatial information by responding in a concentration-dependent manner. Wnts are hydrophobic due to their multiple posttranslational lipid modifications, but surprisingly, they are able to travel up to 20 cell diameters to communicate with their targets [141]. For this reason, it is believed that Wnts are mobilized by special trafficking mechanisms that solubilize the protein and allow it to freely diffuse. For example, Wnts are thought to be exported as micelle-like complexes or secreted on lipoprotein particles [141]. Additionally there is evidence that cell surface heparan sulfate proteoglycans bind Wnts to distribute the protein laterally from cell to cell [141].

1.4b Non-canonical Wnt signaling

Wnt signaling has historically been divided into two major categories: the so-called canonical, or β -catenin dependent pathway and the non-canonical, β -catenin independent pathway. Wnt5a, a non-canonical Wnt, can signal by inhibiting the canonical pathway to influence transcription or via the calcium/protein kinase C (PKC) and planar cell polarity (PCP) pathways to stimulate migration and polarity [142, 143] (**Figure 1.3**). In the calcium/PKC pathway, Wnts signal through Frizzleds to activate Dishevelled (Dvl) and G-proteins that trigger a release of calcium from the endoplasmic reticulum [143]. The increased intracellular calcium activates PKC, which promotes invasion and metastasis through its down stream targets [144-147]. The PCP pathway, active in developing tissues, refers to the polarization of epithelial cells within a plane orthogonal to the apical-basal axis [143, 148]. The exact mechanisms of PCP are not completely understood, but Dvl and Vangl2 [149] are considered key players.

1.4c Wnt5a Receptors

The calcium/PKC and PCP pathways both signal through frizzleds and Ror2 and the pathways likely have some degree of overlap. At this time it is unclear which pathway or receptor(s) are responsible for Wnt5a-stimulated cardiomyocyte migration but we do know that Fzd2 and Ror2 are required for OFT septation (**Table 1.3**) and that both of these receptors are expressed by hESC-CMs (**Figure S2.4F**). Here I will discuss what is known about Wnt5a signaling via these receptors in other systems and will cite examples from both the calcium and PCP pathways when possible. (See **Figure 1.3** for overview).

Fzd2. Frizzleds are seven-pass transmembrane receptors belonging to the family of G-protein coupled receptors (GPCRs) [150]. Although some frizzled actions are pertussis toxin sensitive [151, 152], direct interaction of these receptors with heterotrimeric G-proteins is lacking [150]. Instead, Dvl is believed to be the central component of frizzled-induced signal transduction and is necessary for the canonical, calcium and PCP pathways [150]. Dvl, which directly interacts with the KTxxxW domain in the C terminus of frizzled, is phosphorylated when Wnts bind frizzleds at their extracellular cysteine rich domain [150]. Of the 10 mammalian frizzleds, there is experimental evidence of frizzleds 2, 5 and 7 transducing a Wnt5a signal [153].

It has recently been proposed that Wnt5a signals through Fzd2 to cooperate with integrins and control cell migration and adhesion [121]. Wnt5a regulates these dynamics through Dvl, which localizes with Fzd2 and integrin β 1 at the leading edge of polarized, migrating cells and is required for JNK-dependent phosphorylation of focal adhesion proteins [121].

Ror2. Ror2 (Receptor tyrosine kinase-like Orphan Receptor 2) is a single pass transmembrane protein with a tyrosine kinase domain that binds Wnt5a through its cysteine rich domain. During development Ror2 plays an important role in mediating both chemoattraction and cell polarization in response to Wnt5a gradients. For example, mesenchymal cells in the developing mouse palate migrate toward a source of Wnt5a in a Ror2 dependent manner [154]. In contrast, a gradient of Wnt5a in the developing limb bud establishes a proximal-distal axis in a field of chondrocytes without inducing cell motility [149]. In this scenario Wnt5a dose-dependently induces Vangl2 phosphorylation via Ror2, essentially creating a Vangl2 activity gradient along the proximal-distal axis. Activated Vangl2 proteins then aggregate on the proximal side of each chondrocyte to establish unidirectional polarity [149].

The examples of Ror2-dependent migration and polarization above involve cells acting in response to a concentration gradient of Wnt5a. Interestingly, a uniform concentration of Wnt5a can also stimulate cell polarity if a second, “instructive” polarizing cue is present [155, 156]. For example, Wnt5a will regulate the formation of lamellipodia at a wound edge, where the loss of cell contact acts as the polarizing stimulus, but has no effect on cells in a confluent monolayer [155].

It is worth noting here that homo-dimerization of this receptor tyrosine kinase by Wnt5a or a dimerizing antibody results in auto-phosphorylation or phosphorylation of other downstream substrates. While this has a demonstrated effect on osteoblast differentiation [157, 158], to date homo-dimerization has not been associated with cellular migration or polarization.

Fzd2 and Ror2 as co-receptors. Above are examples of Fzd2 and Ror2 working in isolation, but recent experimental evidence indicates that in some cases both receptors are required to transduce the Wnt5a signal. For instance, in the prostate cancer cell line DU145,

Wnt5a-stimulated migration and invasion are dependent on expression of both Ror2 and Fzd2 acting through the calcium/PKC pathway [147]. Interestingly, in vitro studies have shown that Ror2 associates via its cysteine rich domain with Fzd2 [116] but the significance of this interaction is unknown.

1.4d Wnt Signaling in Infarcted Myocardium

Many recent studies have shown that canonical (β -catenin dependent) Wnt signaling modulates fibrosis in infarcted heart tissue (reviewed in [139, 159]). Inhibition of this signaling pathway by secreted frizzled related protein 2 (SFRP2) reduces collagen deposition and infarct size and improves cardiac function in animal models of myocardial infarction [160, 161]. Similarly, treatment of infarcted mouse hearts with the Frizzled 1/2 antagonist, UM206 reduces collagen deposition and fibrosis while increasing myofibroblast numbers in the infarct area [162]. Additionally, treatment with this molecule improved functional markers such as end diastolic volume and ejection fraction and prevented death due to heart failure (which was 35% in control animals at 5 weeks post-infarct). Because this molecule reversed the inhibitory effect of Wnt3a (a canonical Wnt) on fibroblast migration and differentiation in vitro, it is believed that UM206 exerted the observed in vivo benefits by inhibiting the β -catenin dependent pathway [162].

Taken together this evidence suggests that inhibition of canonical Wnt signaling could serve as a therapeutic approach to prevent adverse cardiac remodeling following infarct. As mentioned above, Wnt5a is known to inhibit canonical Wnt signaling both by competing for Frizzled receptors and by inhibiting β -catenin dependent transcription via Ror2 [153]. The effect of Wnt5a on cardiac remodeling is unknown, but it is interesting to speculate that

exogenous addition of this molecule could serve a dual purpose; promoting migration of engrafted cells and reducing fibrosis.

1.5 Thesis Overview

An improved understanding of the factors that regulate hESC-CM migration would be valuable for two practical reasons: 1. Pro-migratory extracellular matrix proteins or soluble factors could be used to promote migration of engrafted hESC-CMs, perhaps improving their electrical integration with the host. Our lab has demonstrated that hESC-CMs are capable of electrically integrating with host myocardium, but engrafted cells often remain isolated by insulating scar tissue. Above I briefly outlined a strategy to increase the likelihood of host-graft contact by promoting hESC-CM migration within infarcted myocardium. One way to achieve this goal would be to establish a gradient of a chemotactic molecule that would guide hESC-CMs through collagenous scar tissue toward intact host myocardium.

2. A better understanding of cardiomyocyte migration could provide new insights into human heart development. Above I have described ECM and soluble factors that are known to be important for heart morphogenesis, but with a few exceptions their direct role in cardiomyocyte migration has not been shown. It is unclear if these factors are playing a role in migration, proliferation or differentiation or even if they are having their effect on cell types other than cardiomyocytes. This study has the potential to define a biological role for these factors and shed some light on the mechanisms behind these morphogenic processes.

Furthermore, all of the evidence for cardiomyocyte migration above comes from animal model systems such as mouse, chick and zebrafish, so the effect of these molecules on human

cardiomyocytes is not known. hESC-CMs provide a unique opportunity to ask questions about cardiomyocyte biology that cannot be answered in the human fetal system.

This study is the first to describe hESC-CM migration and to identify the factors that regulate this process [1]. **We hypothesized that hESC-CMs would migrate in response to ECM and soluble factors that are important for heart morphogenesis.** In the next chapter I will describe how we tested this hypothesis by screening candidate molecules derived from the development literature and discovered that fibronectin is haptotactic and Wnt5a is both chemokinetic and chemotactic for hESC-CMs. In Chapter 3 I will discuss what these findings mean for cardiac therapy and heart development. I will then describe future experiments that would help to define the role of Wnt5a in the developing outflow tract and to elucidate the mechanism by which this protein drives hESC-CM migration. I'll end by suggesting future work to be performed in vitro that will prepare us to test the hypothesis that guided hESC-CM migration can improve electrical integration following intra-cardiac transplantation.

Secondary Septum-Formed from inward folding of the atrial roof. Fusion of the primary and secondary septums close the ostia secundum at birth.

Primary Septum-A muscular outgrowth from the atrial roof lead by the mesenchymal cap (not shown). Note the mesenchymal cap muscularizes when it fuses with the DMP and AV cushions, closing the ostia primum.

DMP (Dorsal Mesenchymal Protrusion)-Protrudes into the atrial chamber from the SHF dorsal to the heart tube.

AV septum-Derived from fusion of superior and inferior cushions, DMP, mesenchymal cap of the primary atrial septum and the IVS.

Tricuspid Valve-Derived from right lateral, superior and inferior cushions.

Mitral Valve-Derived from left lateral, superior and inferior cushions.

Ventricular Trabeculae-Formed from delamination and migration of cardiomyocytes from compact muscle into sub-endocardial cardiac jelly.

IVS (Interventricular Septum)-Formed from ballooning and inward folding at the apex of the ventricle.

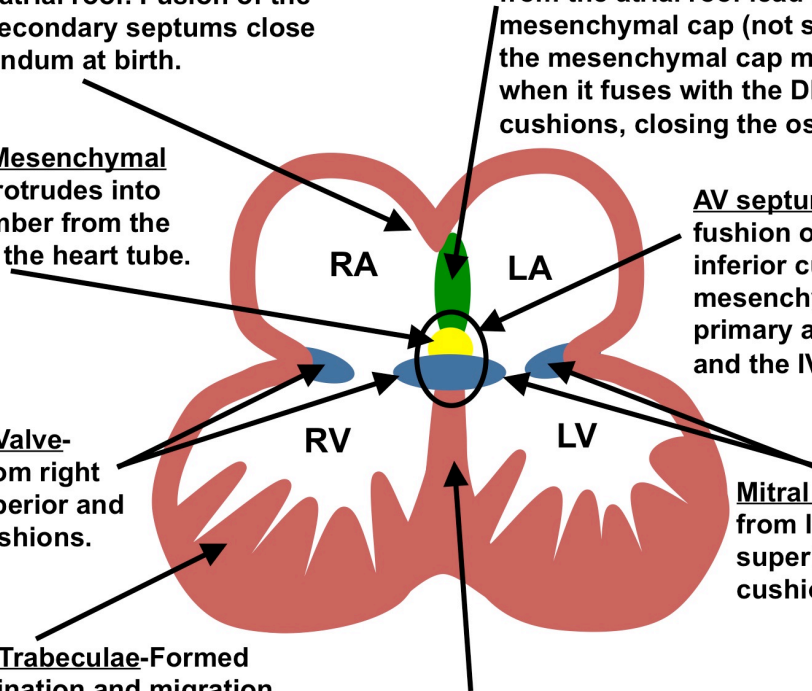
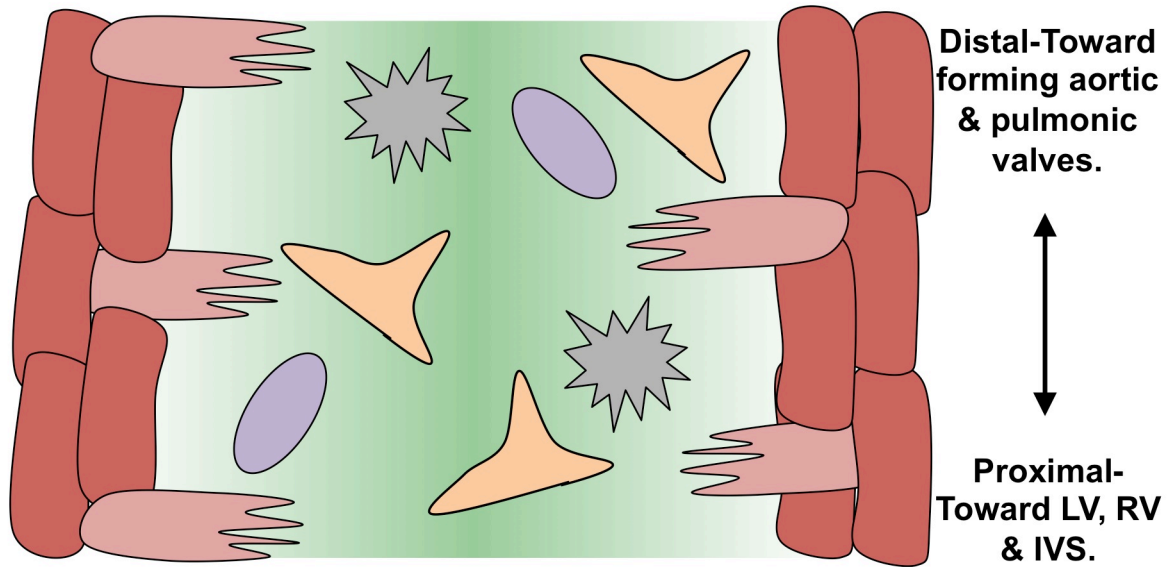
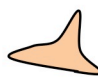
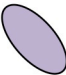

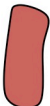
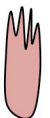



Figure 1.1 Illustration of the valves and septal structures of the mature heart. For each structure, there is a brief description of its formation and the tissue from which it was derived. Modified from [103, 104, 106].



-  **Endocardial-Derived Mesenchymal Cell**-Cells that have undergone EMT & invaded the cardiac jelly to populate the OFT cushions initially.
-  **Cardiac Neural Crest Cell (CNC)**-Migrate from the neural crest (from top of diagram) into the cushion mesenchyme during OFT septation.
-  **Apoptotic Cell**-Cells within the cushion undergo apoptosis as cardiomyocytes begin to invade.
-  **Cardiomyocyte** in the proximal OFT myocardial layer. These cells are derived from SHF and express Fzd2*, and PCP pathway components Vangl2, Wnt11 and Dvl2.
-  **“Myocardializing”** Cardiomyocyte undergoing EMT and invade the mesenchymal endocardial cushion. What sets these apart from the cells above is unknown, but Vangl2 and FAK are required for lamellipodial extension.
-  **Wnt5a Gradient**-Cardiomyocytes in the myocardial layer respond to a chemotactic gradient** of Wnt5a and invade the mesenchymal septum to create a muscular OFT septum.

*Yu et al showed that Fzd2 is localized to the proximal OFT at E13, but it's cell-specific expression was not determined.

**Wnt5a message is found in the mesenchyme tissue at E10.5 and 12.5. The expressing cell type and the significance of the Wnt5a ligand are unknown.

Figure 1.2 Proposed mechanism for Wnt5a-stimulated myocardialization of the OFT septum. Note, at this time point (approximately E12.5) the mesenchymal endocardial cushions have fused with each other and the interventricular septum, dividing the left and right side of the heart. Modified from [115].

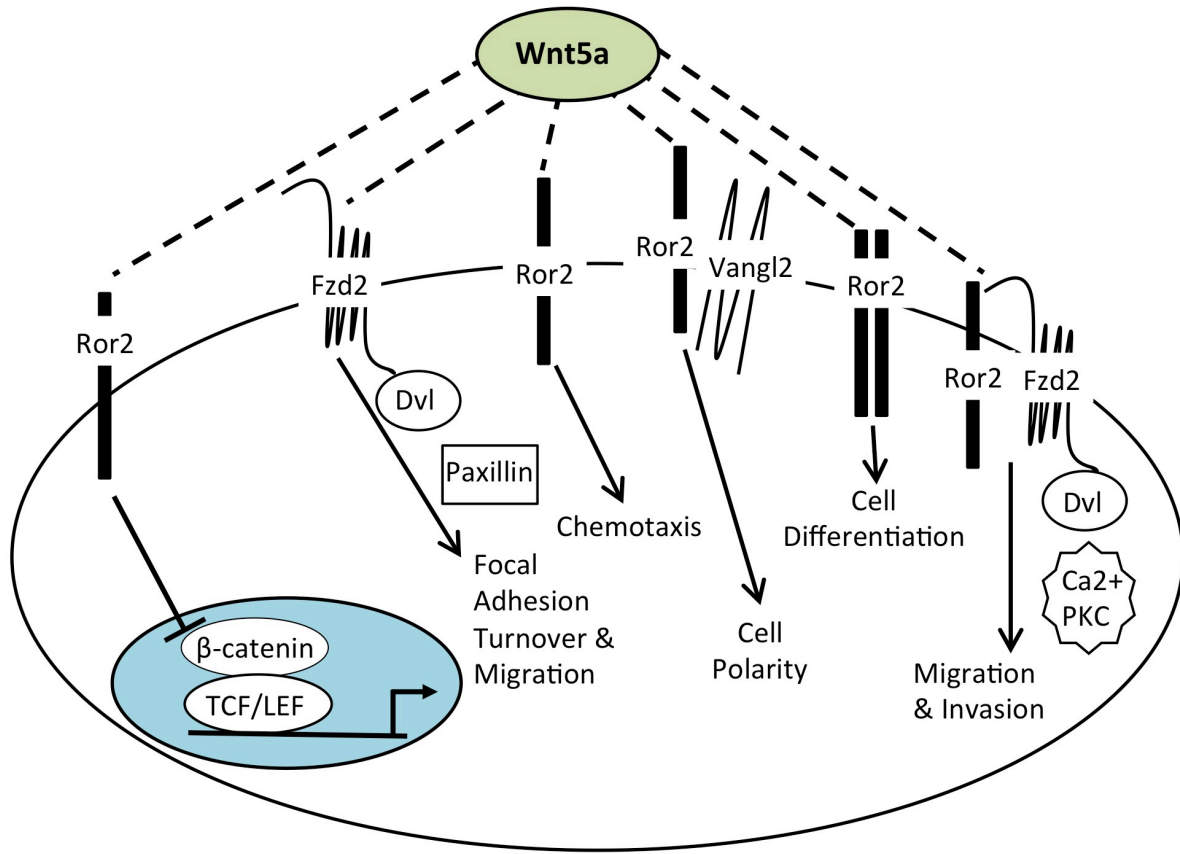


Figure 1.3 Wnt5a signals through Fzd2 and Ror2 to regulate transcription, differentiation, migration and polarity. More details are available in section 1.4. Modified from [142, 153, 163].

Lab	Protocol	Rationale	Purity
Mummery & Davidson	Embryoid bodies are treated with END-2 (endodermal cell line) conditioned media & small molecule inhibitor of p38 MAP kinase.	Anterior endoderm has a cardio-inductive effect. p38 MAP kinase blocks cardiomyogenesis and commits cells to neuronal lineages.	~22%
Murry, Laflamme & Geron Corporation	Monolayers are treated with serial application of Activin A & BMP4.	Activin A promotes induction of mesendoderm in the epiblast. BMP4 induces cardiogenesis in pre-cardiac mesoderm.	30-60%
Palecek	Monolayers are treated with serial application of Activin A & BMP4 without insulin.	Inductive capacity of Activin/Nodal is suppressed by insulin/phosphatidylinositol 3-kinase signaling.	30-80%
Keller	Embryoid bodies are treated with BMP-4, bFGF, and activin A then dissociated, seeded in a monolayer and treated with Dkk1.	BMP-4, bFGF, and activin A induce a primitive streak-like population. Dkk prevents inhibitory actions of Wnt signaling on cardiogenesis.	40-50%
Kamp	Monolayers are sandwiched in matrigel prior to treatment with Activin A, BMP4 and bFGF.	Matrigel promotes the epithelial to mesenchymal transition that epiblast cells undergo during gastrulation. Activin A promotes induction of mesendoderm in the epiblast. BMP4 and bFGF induce cardiogenesis.	98%
Palecek	Monolayers are treated with a GSK3 inhibitor to induce Wnt signaling followed by an inhibitor of porcupine that prevents Wnt production.	Wnt has a biphasic effect on cardiogenesis. It is required for early mesoderm induction, but it inhibits the cardiac induction of pre-cardiac mesoderm at later time points.	80-98%

Table 1.1 Methods for differentiating cardiomyocytes from hESCs. Investigators have taken lessons from embryonic development to direct the differentiation of hESC-CMs from pluripotent stem cells. GSK, Glycogen Synthase Kinase.

	Heart Field Formation	Heart Tube Closure	Addition of SHF
Chick	HH5-HH8	HH9-HH11	HH14-HH20
Mouse	E7-E8	E8-E9	E8-E9
Human	Day 18	Day 28-29	Day 28-33
Candidate Molecule?	N/A	<u>FN</u> is required for heart tube fusion of early CMs.	N/A

	Trabeculation	Chamber Septation	Myocardialization
Chick	HH16-HH17	HH15-34	HH28
Mouse	E10.5	E9-E14.5	E12-E13
Human	Day 30	Day 33 onward	Day 39-43
Candidate Molecule?	<u>NRG1</u> is required for CMs to populate cardiac jelly.	<u>ColVI</u> and <u>DSCAM</u> overexpression lead to ASD.	<u>Wnt5a & 11</u> necessary for OFT septation.

Table 1.2 Time line for the morphogenetic events from heart field formation to myocardialization of the proximal OFT septum. Candidate pro-migratory factors are underlined. Developmental stages are taken from [78, 103, 104, 111]. The wider range is given where there are discrepancies in the literature. HH, Hamburger Hamilton developmental stage; E, Embryonic Day; FN, Fibronectin; SHF, Secondary Heart Field; NRG, Neuregulin; ColVI, collagen VI; DSCAM, Downs Syndrome Cell Adhesion Molecule; ASD, Atrial Septal Defect; OFT, Outflow Tract.

Knock Out	Septal Defect	Expression Pattern	CNC Involvement	SHF Involvement	Myocardialization Abnormalities
Wnt5a	PTA w/ sub-aortic VSD [116, 122]	-Myocardium of OFT[122] -Endocardial Cushion [113] -Secondary heart field [122]	-Initial migration of CNC normal -Lack of PlexinA2 CNC in OFT [122]	-Normal formation of SHF -Addition of SHF cells to OFT not examined [122]	Not examined
Wnt11	PTA w/ sub-aortic VSD [123]	Myocardium of OFT [113]	Migration of CNC normal[123]	SHF lineages present[123]	Failure of CM to extend lamellipodia into cushion, dependent on TGFβ2[123]
Fzd1/2	OFT & VSD defects [119]	-Neonatal CMs (Fzd2) [164] -Ventricle (Fzd2) [165], -OFT (Fzd1/2) [119]	Not examined	Not examined	Not examined
Dvl2	OFT defects [120]	Myocardializing CMs[113]	Attenuated expression of CNC markers[120]	Not examined	Not examined
Dvl3	PTA [166]	OFT [166]	No abnormalities [166]	No abnormalities [166]	Not examined
Ror2	PTA & VSD[116, 163]	Developing heart[116, 117]	Not examined	Not examined	Not examined
Vangl2	Impaired myocardialization of OFT [113]	OFT myocardium [113]	No abnormalities [167]	Not examined	Failure of CM to extend lamellipodia into cushion[113]
FAK (Nkx2.5+ cells)	Impaired myocardialization & other OFT defects [114]	Developing heart[114]	Not examined	Not examined	Failure of CM to extend lamellipodia into cushion[114]

Table 1.3 Non-canonical Wnt signaling is critical for outflow tract septation. The phenotypes of some Wnt-associated knockout mice are listed here. Successful septation involves addition of SHF cells to the OFT, CNC migration and myocardialization of the cushion mesenchyme. Because these highly coordinated processes involve many cell types, the mechanism contributing to septal defect is often unclear. Knockout of Wnt5a and its receptors, Fzd2 and Ror2, result in OFT septation defects that could partially be explained by aberrant cardiomyocyte migration during myocardialization. CM, cardiomyocyte; CNC, cardiac neural crest; PTA, persistent truncus arteriosus; OFT, outflow tract; SHF, secondary heart field; VSD, ventricular septal defect.

Chapter 2: hESC-CMs Migrate in Response to Gradients of Fibronectin & Wnt5a

2.1 Summary

Human embryonic stem cell-derived cardiomyocytes (hESC-CMs) have attracted considerable interest as both a model for human heart development and a potential source for regenerating infarcted heart tissue. As described below, hESC-CMs exhibit significant spontaneous migratory activity in vitro. To our knowledge, this phenomenon has not been previously reported, nor is it known what signaling molecules might modulate their migration. While adult cardiomyocytes are not considered a particularly migratory cell type, the motility of immature cardiomyocytes such as hESC-CMs is not unexpected. Indeed, it is well-established that a number of critical steps in heart development involve cardiomyocyte migration, including heart tube closure [86], muscularization of the outflow tract [115], as well as septation [114] and trabeculation [94] of the ventricles, but the chemotactic cues driving these processes remain incompletely defined. Pro-migratory factors have been identified for related cell types including skeletal myoblasts [168] and adult cardiac progenitors [169, 170], but it was unknown whether hESC-CMs would respond to these same factors.

An improved understanding of the conditions and signaling molecules that affect hESC-CM migration would have significant practical value. First, nearly all current knowledge regarding cardiomyocyte motility has come from developmental studies in non-human model systems. The hESC-CM system represents a unique opportunity to study this behavior in human cardiomyocytes. Second, while the transplantation of hESC-CMs improves contractile function in preclinical infarct models, our group has shown the electromechanical integration of hESC-CM grafts is limited in injured hearts because many of the implants are isolated by scar tissue [171]. We speculate that, by stimulating their migration in vivo, one might be able to direct

engrafted hESC-CMs toward the border zone, thereby increasing the likelihood of host-graft contact and electromechanical coupling.

To identify molecules that promote hESC-CM migration, we took a candidate factor approach and used the relatively high-throughput transwell assay to test molecules known to either be involved in cardiac morphogenesis [84, 86, 94, 97, 108, 116, 122, 123, 172-176] or the migration of myoblasts [168] or adult cardiac progenitors [169, 170]. We then validated our transwell findings using the two-dimensional haptotaxis and chemotaxis assays, as well as the gap closure assay. Based on these studies, we conclude that hESC-CMs sense and migrate in response to gradients of FN, an extracellular matrix (ECM) glycoprotein, and Wnt5a, a non-canonical Wnt ligand [1].

2.2 Materials and Methods

Reagents, Antibodies and Immunostaining. Type 1 rat tail collagen (hereafter abbreviated as Col I), human plasma FN and vitronectin (VN) were all purchased from Invitrogen (Grand Island, NY). Placental laminin (LN) was purchased from Sigma (St Louis, MO) and Type VI collagen from BD Biosciences (San Jose, CA). For all coating procedures, FN, VN, LN and Col VI were diluted in calcium free PBS, and Type 1 rat collagen was diluted in 0.2N acetic acid. Tissue culture plates were first coated overnight at 4°C with 0.1% polyethyleneimine (PEI, Sigma), rinsed three times with water and then coated for 1 hour at 37°C with ECM protein at varying concentrations. For the gap closure and Wnt5a-stimulated live-cell microscopy assays, wells were coated with PEI followed by FN at 2.5 $\mu\text{g}/\text{cm}^2$ (10 $\mu\text{g}/\text{mL}$, 0.5 mL per well of a 24-well plate). All surfaces were rinsed with PBS, aspirated and stored dry at 4°C until use.

Anti-integrin α -5 (#Ab23589, Abcam, Cambridge, MA) and anti-integrin α -V (#Ab16821, Abcam, Cambridge, MA) were used at 5 μ g/mL for integrin blockade. For these studies, hESC-CM migration was quantified by immunostaining with rabbit anti-cTnT at 1:200 (#Ab91605, Abcam, Cambridge, MA). For all other transwell experiments and for quantification of cardiac purity, we used mouse anti-cTnT at 1:200 (#MS-295-P, Thermofisher, Waltham, MA).

L-cell Conditioned Media. Control L-cells and L-cells overexpressing Wnt5a [177] (ATCC, Manassas, VA) were cultured in 20 mL of DMEM containing 10% fetal calf serum (FCS) and 1% penicillin/streptomycin per 150 cm² dish. Once cells were confluent, FCS was reduced to 5% and media was collected every 48 hours for 6 days. The resultant conditioned media was centrifuged at 3000 X g for 15 minutes at 4°C to pellet cell debris. Supernatants were stored at 4°C for up to 3 weeks.

hESC-CM Derivation and Purification All experiments were approved by the University of Washington's Embryonic Stem Cell Research Oversight Committee (ESCRO) and involved the H7 hESC line (Wicell Research Institute, NIH Stem Cell Registry #hESC-10-0061). In brief, undifferentiated hESCs [7] were expanded in mouse embryonic fibroblast-conditioned medium (MEF-CM) supplemented with basic fibroblast growth factor [11]. To induce cardiogenesis, we treated compact monolayers of hESC with serial activin A and BMP-4 as previously described [3, 178] (**Supporting Information Fig. S2.2.1A**). For the initial transwell screens of ECM and soluble factors, we used non-selected hESC-CM populations of ~60% cardiomyocyte purity [171, 179]. For all other experiments, we used highly enriched hESC-CM preparations obtained via genetic selection. For this, we created a lentiviral vector in which regulatory elements from the striated muscle-specific muscle creatine kinase (MCK)

promoter [180] drive expression of the fluorescent protein, mCherry, and puromycin resistance (**Supporting Information Fig. S2.1B**). We transduced differentiating hESC-CM cultures with this vector on day 5 post-induction with activin A and then applied puromycin selection (2.5 $\mu\text{g/ml}$) on day 22 for 48 hours. This protocol yielded cell populations that were 99% positive for both mCherry and the cardiac marker, cardiac troponin T (cTnT), which were then used for migration studies (**Supporting Information Fig. S2.1C-E**).

Transwell Assay. For all transwell experiments, we used light-opaque transwell inserts with 8 μm diameter pores and a growth area of 0.3 cm^2 (BD Falcon Fluoroblok, BD Bioscience, San Jose, CA). For the ECM checkerboard experiments, we exposed each face of the membrane to 0.25, 2.5 or 25 $\mu\text{g/cm}^2$ of dissolved proteins (which corresponded to a 75 μl volume of 1, 10 or 100 $\mu\text{g/mL}$ ECM concentration) for 5 minutes at room temperature. At lower ECM concentrations, hESC-CMs typically failed to adhere. For all other transwell experiments, the top and the bottom of the membrane were both coated with 25 $\mu\text{g/cm}^2$ FN for 5 minutes at room temperature. After coating, membranes were aspirated, rinsed with PBS and stored dry at 4°C until use. We seeded 7.5×10^5 hESC-CMs per transwell and allowed 14 hours for initial adhesion before exposing the cells to a particular set of experimental conditions (e.g. treatment with a candidate growth factor). To determine the number of cells present on either side of the membrane after the specified interval of time under these conditions, we fixed the membranes with 4% paraformaldehyde and then immunostained them with an antibody against cTnT (with detection by an Alexa 488-conjugated secondary antibody). A blinded observer used an Olympus IX71 inverted epifluorescence microscope to count the number of cTnT+ cardiomyocytes on either side of the membrane, using at least eight 10X fields. To account for any migration that may have occurred during the initial seeding period, we also immunostained

equivalently prepared membranes that were fixed at this time-point and used these counts to correct the experimental groups. Migration across the transwell was then expressed either as the percentage of attached cardiomyocytes that had migrated to the bottom of the membrane ($100 \times \text{bottom} / (\text{top} + \text{bottom})$) or as the ratio of migrated cardiomyocytes under treated versus control conditions (i.e. fold over control).

Formation of Surface-Bound Fibronectin Gradients. To generate reproducible gradients of FN on two-dimensional glass surfaces, we employed the agarose diffusive printing method previously described by Mai et al [181]. In brief, we used standard photolithographic techniques to fabricate a silicon wafer mold. To create the “stamp”, we poured a 3% agarose solution over the latter mold and allowed it to solidify for 30 minutes (**Supporting Information Fig. S2.2A, Step I**). Next, we transferred the resultant patterned agarose stamp to a 0.1% PEI-coated glass-bottom dish (MatTek, Ashland, MA), punched holes on either side of the grid to access the channels and then loaded the channels with 10 μL of Oregon 488-conjugated FN (Life Technologies, Grand Island, NY) at 850 $\mu\text{g}/\text{mL}$ (**Supporting Information Fig. S2.2A, Step II**). As it diffused through the gel, the fluorescently-tagged FN deposited onto the underlying glass surface (**Fig. 2.3A-B, Supporting Information Fig. S2.2B**). Reproducible steep or shallow gradients of surface-bound FN were formed by allowing the molecule to diffuse through the gel for 20 or 60 minutes, respectively (**Fig. 2.3C**). The agarose stamp was then removed prior to cell seeding (**Fig 2.3D**).

To quantitate the relative slope of the two surface-bound FN gradients, we used a Zeiss AxioObserver epifluorescence microscope equipped with an AxioCam CCD to image Oregon 488-FN gradients formed with 20 or 60 minutes of diffusion time. The resultant fluorescent signal intensity was then analyzed using Image J software. The steep FN gradients (20 minutes

of diffusion time) showed a fluorescence intensity (F.I.) slope of 123 ± 7 arbitrary units (A.U.) per μm versus 77 ± 4 A.U. per μm for the shallow gradients (60 minutes of diffusion) ($p < 0.01$, $n=3$). We calibrated these fluorescent signals by comparison with surfaces coated with known concentrations of Oregon 488-FN and estimated that the steep and shallow gradients had slopes of ~ 7.4 and $4.6 \mu\text{g}/\text{cm}^2$ FN per $100 \mu\text{m}$ distance, respectively. During live-cell microscopy experiments, we limited our analysis to cells in the linear portions of the FN gradient (i.e. the first $200 \mu\text{m}$ of the steep gradient and the first $325 \mu\text{m}$ of the shallow gradient.) This corresponded to coating densities in the range of ~ 2.5 to $15 \mu\text{g}/\text{cm}^2$ FN.

Live-Cell Migration Analysis. To observe the migration of genetically-selected, mCherry+ hESC-CMs on two-dimensional surfaces, we used an automated inverted microscope (Nikon Eclipse Ti) equipped with a humidified environmental chamber (37°C , $5\%\text{CO}_2$) and an Andor iXon+ EM-CCD camera. Time-lapse images were acquired every 15 minutes and were analyzed with Nikon Elements Image Analysis Software by tracking the change in the position of the centroid of the cell at each time point. Cell speed was calculated as path length (distance in μm) divided by time (hours). Net migration was calculated in both parallel and perpendicular directions relative to the applied gradient.

Gap Closure Assay. We seeded genetically selected, mCherry+ hESC-CMs into a commercially-available tissue culture insert (Ibidi, catalogue # 80209, Munchen, Germany) and cultured them until a confluent monolayer was formed (approximately 24 hours). We then removed the insert, leaving a highly reproducible $500 \mu\text{m}$ wide gap. Images were acquired both immediately after removal of the insert and following an additional 24 hours of culture under control or Wnt5a-stimulated conditions. Gap closure was calculated by subtracting the gap area at the 24-hour time-point from the starting gap area (measured using Image J software).

Chemotaxis Assay of Diffusive Wnt5a Gradient. To determine the chemotactic response of hESC-CMs to Wnt5a, we used a commercially-available, microfluidics-based chemotaxis device (iBidi 2D chemotaxis chamber, #80301, Munchen, Germany) as per the manufacturer's protocol. Based on a previously published characterization of this device, one would expect a linear gradient of Wnt5a to be formed within several hours and to remain stable for at least 48 hours [182]. For our experiments, we coated the cell viewing chamber of this device with FN ($15 \mu\text{g}/\text{cm}^2$) for 1 hour at 37°C and then rinsed multiple times with PBS. We then seeded genetically selected, mCherry+ hESC-CMs into the viewing chamber and allowed the cells to adhere overnight in control conditioned media (C-CM). The next day, we loaded fresh C-CM and Wnt5a-CM into reservoirs located on either side of the cell viewing chamber. Live-cell imaging was then performed as detailed above, allowing 12 hours for the Wnt5a gradient to form and then tracking cardiomyocyte migration over the following 48 hours.

RT-PCR assays. Genetically-selected hESC-CMs were cultured on FN for 72 hours and then were lysed for the isolation of total RNA (Qiagen RNeasy kit). mRNA was reverse transcribed using the Superscript III first-strand cDNA synthesis kit and oligo(dT) primers (Invitrogen). PCR was performed for 30 cycles using previously validated primer sequences (see **Tables 2.2 & 2.3**).

Statistics. Statistical analyses were performed using Graphpad Prism (La Jolla, CA) with the threshold for significance set at level $p < 0.05$. Values are expressed as mean \pm standard error. To compare migration speed of hESC-CMs on the four different coating densities of each ECM protein, we used the Kruskal-Wallis method followed by the Dunn's post-hoc for all pairwise comparisons. ECM transwell experiments were analyzed by one-way ANOVA followed by Tukey's post-hoc for all pairwise comparisons then Bonferroni corrected. The

initial transwell screen of soluble factors was analyzed using a one-way ANOVA followed by a Dunnett's post-hoc comparing all experimental samples to control. For all other comparisons, a two sample t-test was used.

2.3 Results

hESC-CMs Migrate Spontaneously on Two-Dimensional Surfaces. To demonstrate the migratory behavior of hESC-CMs in the absence of any exogenously applied cues, we used live-cell microscopy to image genetically-selected, cTnT/ α -actinin expressing hESC-CMs after 25 days of in vitro differentiation. For this, cells were seeded at low density into a glass bottom dish coated with 0.1% PEI followed by FN at $2.5 \mu\text{g}/\text{cm}^2$, allowed to adhere for 16 hours, and then monitored continuously for 24 hours (**Fig. 2.1A-D**). Under these conditions, a majority of individual hESC-CMs exhibited random migration, although their migration speed varied considerably. Of note, this migration occurred despite the fact that the hESC-CMs maintained spontaneous contractile activity throughout. Having made the initial observation that hESC-CMs are motile, we sought to find an ECM molecule and optimal coating density that would induce the fastest rate of migration. For this, we again used live-cell microscopy to track the migration of hESC-CMs cultured on 2D surfaces coated with varying concentrations of FN, Col VI, Col I, VN and LN (**Table 2.1**). While there were some exceptionally fast cells on Col VI, hESC-CMs under most conditions migrated at a range of 2.5-10 $\mu\text{m}/\text{hour}$ with no significant difference in migration between lower and higher concentrations of ECM (**Fig. 2.1E-I**).

hESC-CMs Exhibit a Haptotactic Response to Fibronectin and Other ECM Molecules. After confirming that hESC-CMs show random migration when cultured on surfaces coated with a uniform concentration of each ECM protein, we examined their behavior when exposed

to concentration gradients of these molecules. For this, we employed the "checkerboard" transwell assay after Zigmond et al [183], coating the membranes with symmetric or asymmetric concentrations of FN, Col VI, Col I, VN or LN. hESC-CMs were dispersed to single cells, seeded onto these transwells and allowed to migrate for 16 hours before fixation. We then quantified the absolute number of cTnT+ cardiomyocytes on the bottom of each membrane and expressed migration as fold over control (symmetrically coated FN).

For all of the ECM molecules tested, the number of cells that migrated toward the higher concentration increased with the steepness of the ECM gradient across the membrane. The largest number of migrated cells was found when membranes were coated with FN at a 100-fold concentration difference from top to bottom ($0.25 \mu\text{g}/\text{cm}^2 : 25 \mu\text{g}/\text{cm}^2$) with cells under these conditions showing nearly five-fold greater migration than cells on a symmetrically coated membrane ($25 \mu\text{g}/\text{cm}^2 : 25 \mu\text{g}/\text{cm}^2$) (**Fig. 2.2A**). Moreover, cells on membranes with the 100-fold FN gradient exhibited nearly five-fold greater migration than those on membranes equivalently coated with LN. To correct for variation in seeding efficiency between different ECM molecules and coating densities, we also calculated the percentage of the total number of cTnT+ hESC-CMs adherent to either side of the membrane that had migrated from top to bottom. This analysis yielded qualitatively similar results, with a trend toward increased migration with a steeper gradient of ECM protein (**Fig. 2.2B**).

Adhesion and Migration on Fibronectin is Integrin $\alpha 5$ and αV Dependent. We next wanted to determine the expression profile of integrins that might be involved in the migratory response to FN. Using RT-PCR on RNA isolated from genetically selected hESC-CMs, we found that hESC-CMs express α -integrins 3, 5-7, 11 and V and β -integrins 1, 3, 4 and 5 (**Fig 2.2C, Table 2.2**). Noting that hESC-CMs express two of the known FN receptors, integrins $\alpha 5$

and αV , we sought to determine which receptor was required for hESC-CM migration on FN by quantifying adhesion and migration of hESC-CMs in the presence of neutralizing antibodies directed against integrins $\alpha 5$, αV or both. We found that while neither antibody alone had a statistically significant effect on these parameters, simultaneous incubation with both anti- $\alpha 5$ and αV antibodies resulted in a $55.8 \pm 18.0\%$ reduction in adhesion (**Fig. 2.2D**) and a 1.8-fold decrease in migration by transwell assay (**Fig. 2.2E**).

hESC-CM Migration on Fibronectin is Dependent on Gradient Slope. To better define the haptotactic response of hESC-CMs to FN, we performed live-cell imaging of genetically-selected mCherry+ hESC-CMs cultured on surface-bound FN gradients of varying concentration steepness. To create the surface-bound FN gradients, we applied agarose diffusive printing techniques [181] and showed that the gradient slope could be reproducibly varied by controlling the length of time that Oregon 488-conjugated FN was allowed to diffuse through the agarose gel (**Supplemental Fig. S2.2, Fig. 2.3A&B**). We then compared the behavior of mCherry+ hESC-CMs seeded onto steep versus shallow FN gradients (generated using 20 versus 60 minutes of diffusion time, **Fig. 2.3C**). In all cases, cells showed biased migration toward higher FN concentrations, but those exposed to a steeper FN gradient moved nearly a three-fold greater distance in that direction than their counterparts on shallower gradients ($40.3 \pm 6.3 \mu\text{m}$ versus $15.6 \pm 2.8 \mu\text{m}$ in 24 hours, $p < 0.01$), (**Fig. 2.3D-G**) while there was no significant difference in net movement perpendicular to the gradients.

To look for synergistic effects by ECM molecules on FN-mediated haptotaxis, we used live-cell microscopy to track hESC-CM migration on steep FN gradients to which we had added uniform ColVI at either 0.25 or 2.5 $\mu\text{g}/\text{cm}^2$. We found that the cells on the FN gradient alone tended to migrate further than those on the gradient + ColVI, (40.9 ± 12.3 vs 21.3 ± 6.2 and

25.8 ± 6.4 microns in 24 hours, respectively), although these differences did not reach statistical significance (**Supporting Information Fig. S2.3A-C**). Given that there was no slowing of migration when the two ECMs were presented uniformly (**Fig. S2.3D**), a direct antagonistic effect seems unlikely to account for these findings.

Wnt5a is a Pro-migratory Factor for hESC-CMs. After determining the migratory responses of hESC-CMs to FN and other ECM proteins, we focused on the identification of soluble factors that might promote hESC-CM migration. For this, we initially used the high-throughput transwell assay to screen candidate signaling molecules that had been previously implicated in either heart morphogenesis or the migration of skeletal myoblasts or adult cardiac progenitors (**Table 2.1**). (See **Supporting Information Figure S2.4A** for specifics regarding the timing of growth factor treatment). Interestingly, among the 10 soluble factors tested, only Wnt5a mediated a statistically robust effect on hESC-CM migration. Indeed, when recombinant Wnt5a (100 and 500 ng/ml) was placed in the bottom chamber of the transwell, hESC-CM migration across the membrane doubled relative to control conditions (**Fig. 2.4A**).

To further confirm the pro-migratory effects of Wnt5a on hESC-CMs, we used two independent migration assays to compare media conditioned by Wnt5a over-expressing (Wnt5a-CM) or wild type L-cells (control-CM) [177]. First, we tracked the movement of genetically-selected hESC-CMs by live-cell microscopy and found that myocytes treated with Wnt5a-CM had approximately two-fold greater random migration than their counterparts in control-CM (**Fig. 2.4B**). Second, to test for effects on multicellular preparations of hESC-CMs, we used the gap-closure assay and found that migration into the gap was enhanced approximately two-fold for cultures treated with Wnt5-CM versus control-CM (**Fig. 2.4 C-E**). Importantly, this effect

was not accounted for by changes in cell size, retention or proliferation (**Supporting Information Fig. S2.4B-D**).

We also performed experiments to screen for synergistic effects or signaling interactions between Wnt5a and FN in our system. Although Wnt5a has been reported to alter the expression of integrins and FN in other cell types [184, 185], we did not find any changes in expression of FN or its receptors (Integrins $\alpha 5$, αV , $\beta 1$ and $\beta 3$) in Wnt5a-stimulated hESC-CMs by qRT-PCR (**Supporting Information Fig. S2.4E**). To see if Wnt5a would augment the haptotactic response to FN, we again generated steep surface-bound gradients and tracked hESC-CM migration on these gradients in the presence and absence of Wnt5a (100 and 500 ng/ μ L). We detected no difference in migration relative to the FN gradient during 24-hours of videomicroscopy between control and Wnt-stimulated cells (**Supporting Information Fig. S2.5**).

Wnt5a Promotes hESC-CM Migration through a Frizzled-Dependent Pathway. By RT-PCR, we found that hESC-CMs express multiple receptors and co-receptors for Wnts, including Frizzled (Fzd) proteins 1-4, Fzd 6-9, LRP5, LRP6, Ror2 and Ryk (**Supporting Information Fig. S2.4F, Table 2.3**). Based on insights from cardiac development [119] and migration studies in other cell types [121, 142, 186], we hypothesized that pro-migratory effects of Wnt5a on hESC-CMs are mediated by Fzd2. To test this hypothesis, we performed the gap closure assay in the presence of the Fzd1/2 peptide antagonist, UM206 (100nM) [187], and found that it completely inhibited the effects of Wnt5a stimulation (**Fig. 2.4E**).

Wnt5a is Chemotactic for hESC-CMs. The preceding data demonstrate that Wnt5a exerts a chemokinetic effect on hESC-CMs. To determine whether Wnt5a also acts as a chemoattractive factor, we first employed the "checkerboard" transwell assay, in which Wnt5a-

or control-CM were variably placed on the top or bottom of the membrane. Consistent with a chemotactic effect, we found that the placement of Wnt5a-CM in the lower chamber of the transwell resulted in a 2.2-fold increase in hESC-CM migration to the bottom of the membrane, while symmetric Wnt5a-CM on the top and bottom had only a minor effect (**Fig 2.5A**). As before, this effect of Wnt5a-CM was completely inhibited in the presence of UM206.

To more directly confirm the chemotactic activity of Wnt5a, we used a commercially-available, microfluidics-based device to expose hESC-CMs to a gradient of Wnt5a-CM during live-cell imaging for 48 hours. Interestingly, hESC-CMs exposed to a Wnt5a gradient moved 5.7 times farther in the direction parallel to the gradient (i.e. toward higher Wnt5a) than did cells under control conditions ($42.0 \pm 7.8 \mu\text{m}$ versus $7.4 \pm 9.4 \mu\text{m}$, $p < 0.01$, $N = 20-23$). The two conditions showed no difference in net movement perpendicular to the gradient (see **Figs. 2.5B** for representative paths of hESC-CMs with and without exposure to a Wnt5a gradient, and **Figs. 2.5C & D** for the corresponding displacement vectors).

2.4 Conclusions

While other investigators have described the migration of both immature cardiomyocytes in the developing heart [84, 94, 114, 115, 188] and putative cardiac progenitors in the post-natal heart [169, 170], similar motility has not been previously reported in cardiomyocytes derived from pluripotent stem cells. Here we used highly purified populations of hESC-CMs and found that these cells can migrate at speeds in the range of 5-10 $\mu\text{m}/\text{hour}$. While much slower than highly migratory cell types (e.g. neutrophils at 390 $\mu\text{m}/\text{hour}$) [189], such values are comparable to those previously reported for Chinese hamster ovary (CHO) cells, a commonly used cell type in migration studies and one that obviously lacks sarcomeric

machinery [190]. Indeed, our finding that hESC-CMs migrate while simultaneously exhibiting rhythmic contraction raises interesting questions as to how cytoskeletal reorganization and myofilament crossbridge cycling remain compartmentalized. This same issue has been raised with regard to beating cardiomyocytes undergoing mitosis [191].

In this study, we focused on identifying signaling pathways that might regulate hESC-CM migration and identified two pro-migratory factors: FN, an extracellular matrix glycoprotein, and non-canonical Wnt5a. We showed by transwell and live-cell microscopy that the haptotactic response to FN can be enhanced by increasing the slope of the surface-bound gradient and that migration and adhesion on FN involves both integrins $\alpha 5$ and αV . Both of these integrins were previously shown to be expressed by hESC-CMs in vitro [192]. Wnt5a was the only soluble factor in our screens that promoted hESC-CM migration, and it appears to exert both chemokinetic and chemoattractant effects. Interestingly, both the chemokinetic and chemotactic responses to Wnt5a can be blocked by UM206, suggesting that they are dependent on Fzd1 and/or 2. Future experiments using shRNA against Frizzleds and Ror2 will be required to confirm the specific receptors involved in these responses.

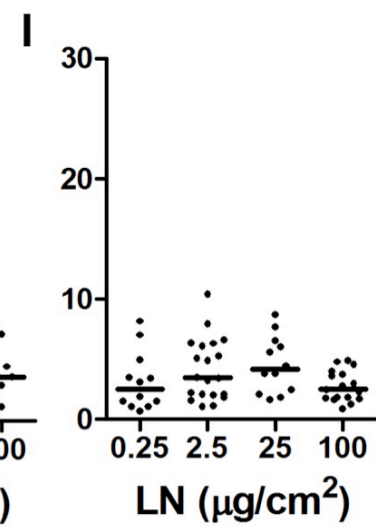
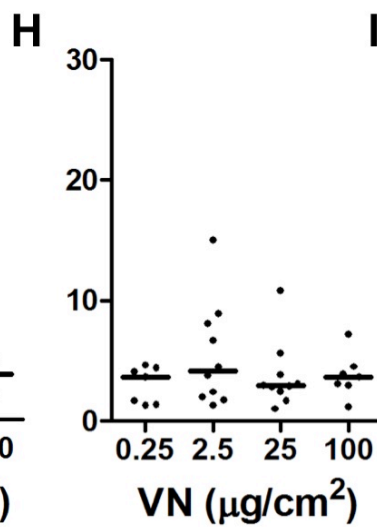
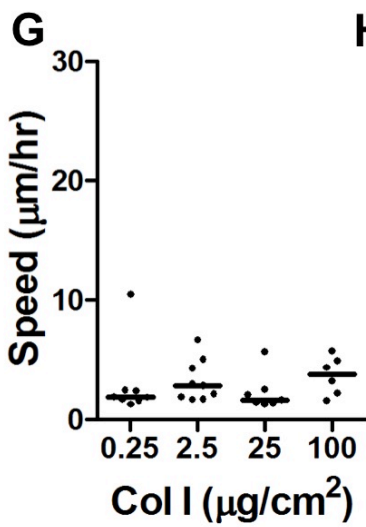
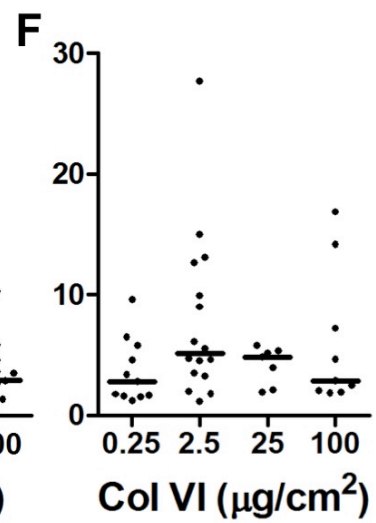
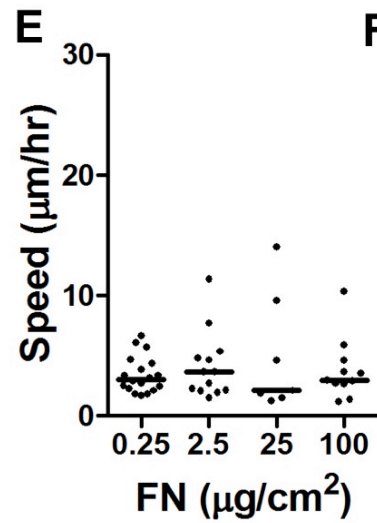
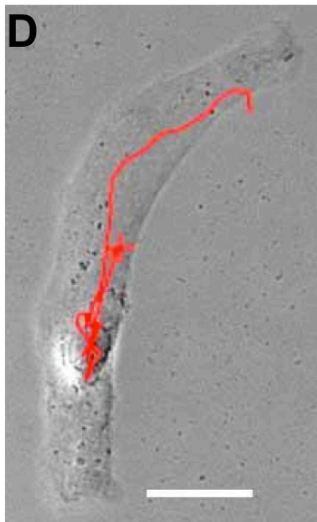
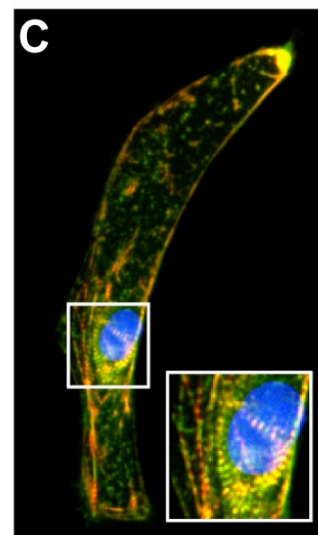
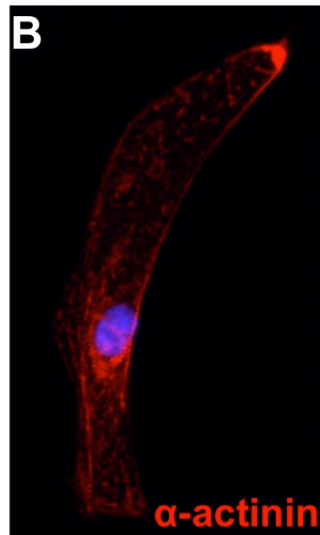
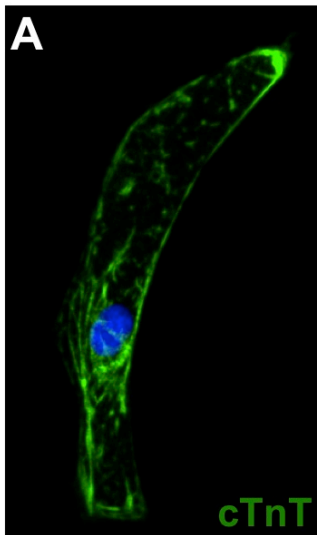


Figure 2.1. hESC-CMs migrate spontaneously on two-dimensional surfaces. (A-C): Immunofluorescent images of the genetically-selected, rhythmically contracting hESC-CMs. Note that this cell expressed the cardiac markers cTnT (**A**, green) and α -actinin (**B**, red). The red trace in (**D**) represents the 24 hour migration path of the centroid of this cell on FN at 2.5 $\mu\text{g}/\text{cm}^2$. Scale bar=50 μm . (**E-I**): Scatterplots showing the migration speed of individual hESC-CMs cultured on FN, Col VI, Col I, VN, LN at the specified coating densities. Bar indicates median. N=7-20 cells per condition.

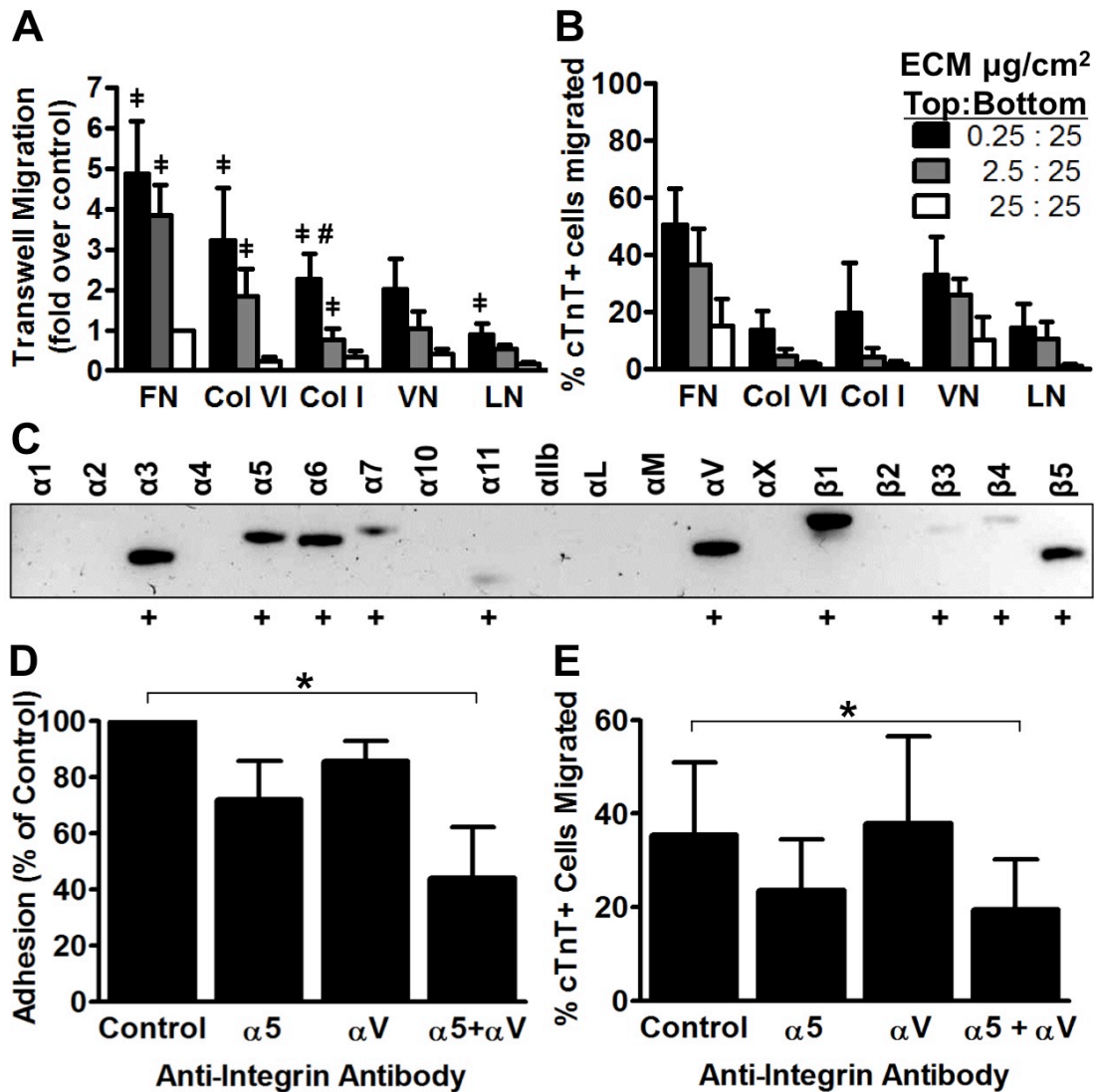


Figure 2.2. hESC-CMs exhibit a haptotactic response to fibronectin. (A): We seeded hESC-CMs onto transwells coated on the top and bottom with varying ECM protein densities and then allowed the cells to migrate for 16 hours. The absolute number of cTnT+ cardiomyocytes detected on the bottom of each membrane was normalized to the symmetrically-coated FN control. † p<0.01 versus 25:25 μg/cm², # p<0.01 versus 2.5:25 μg/cm². N=4. (B): Same experimental samples as in (A), but with migration to the bottom here expressed as a percentage of the total number of cTnT+ cells attached to both sides of the membrane. (C): Integrin expression profile of genetically selected hESC-CMs by RT-PCR. (D, E): hESC-CM adhesion (D) and migration (E) on FN-coated transwells is dependent on integrins α5 and αV. Neutralizing antibodies at 5 μg/mL. N=4, *p<0.05.

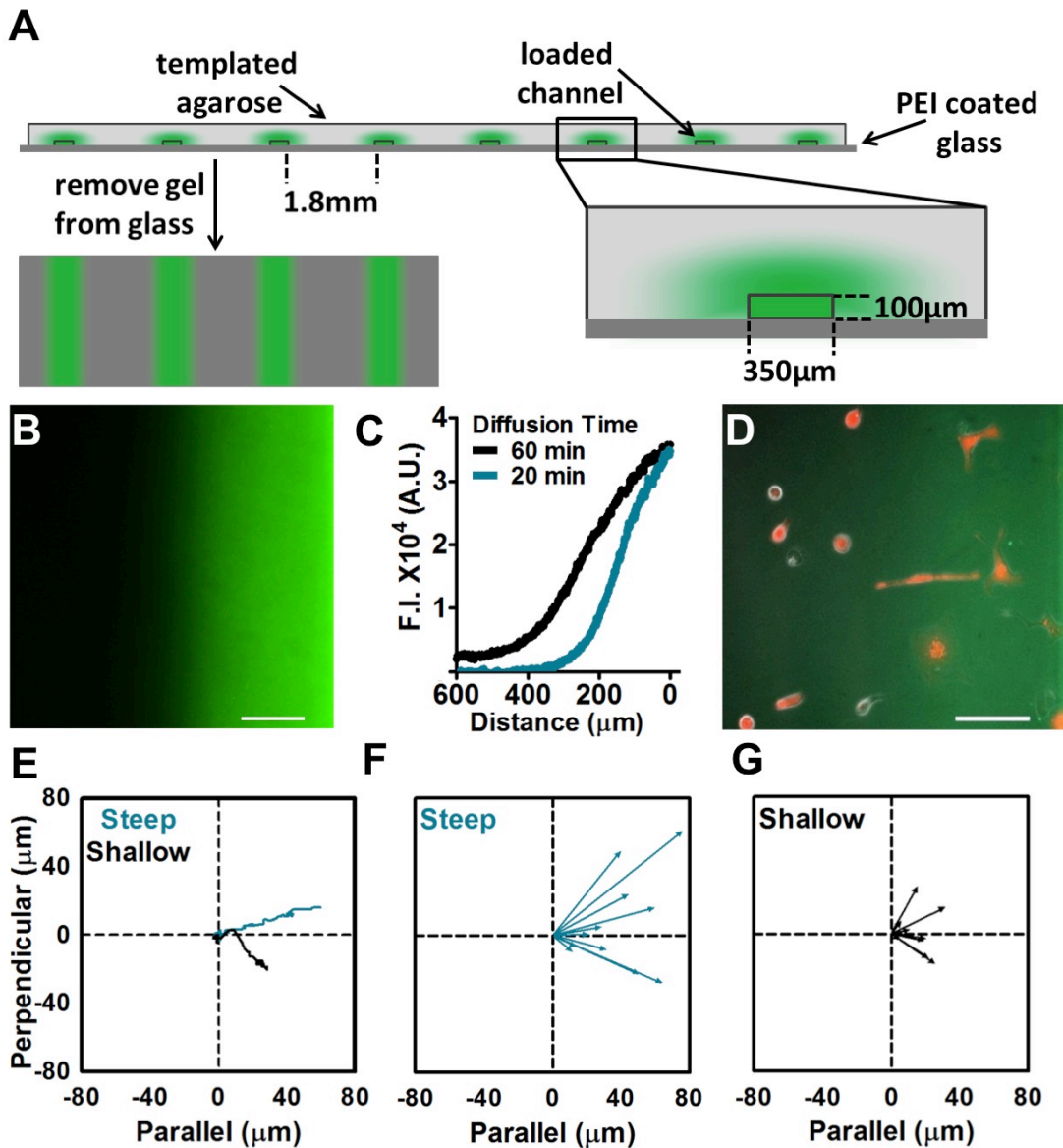


Figure 2.3. hESC-CM migration on fibronectin is dependent on gradient slope. (A): Schematic showing the dimensions of the templated gel and the surface-bound gradient that results from this diffusive printing technique. **(B):** Representative image of a glass-bound gradient of fluorescently tagged FN. **(C):** The steepness of the gradient was varied by changing the diffusion time of the protein through the agarose stamp and quantified using Image J analysis software. (Fluorescence intensity (F.I.) in arbitrary units (A.U.)). **(D):** We calculated the net migration of genetically selected, mCherry⁺ hESC-CMs on these gradients in the direction parallel and perpendicular to the gradient. Only cells within the linear range of the gradient were included in the analysis. Scale bar = 100µm. **(E):** Representative migration paths of hESC-CMs on steep (20 min, blue) and shallow (60 min, black) gradients. Displacement vectors of hESC-CMs on steep **(F)** and shallow **(G)** gradients of FN. N=11 cells per condition.

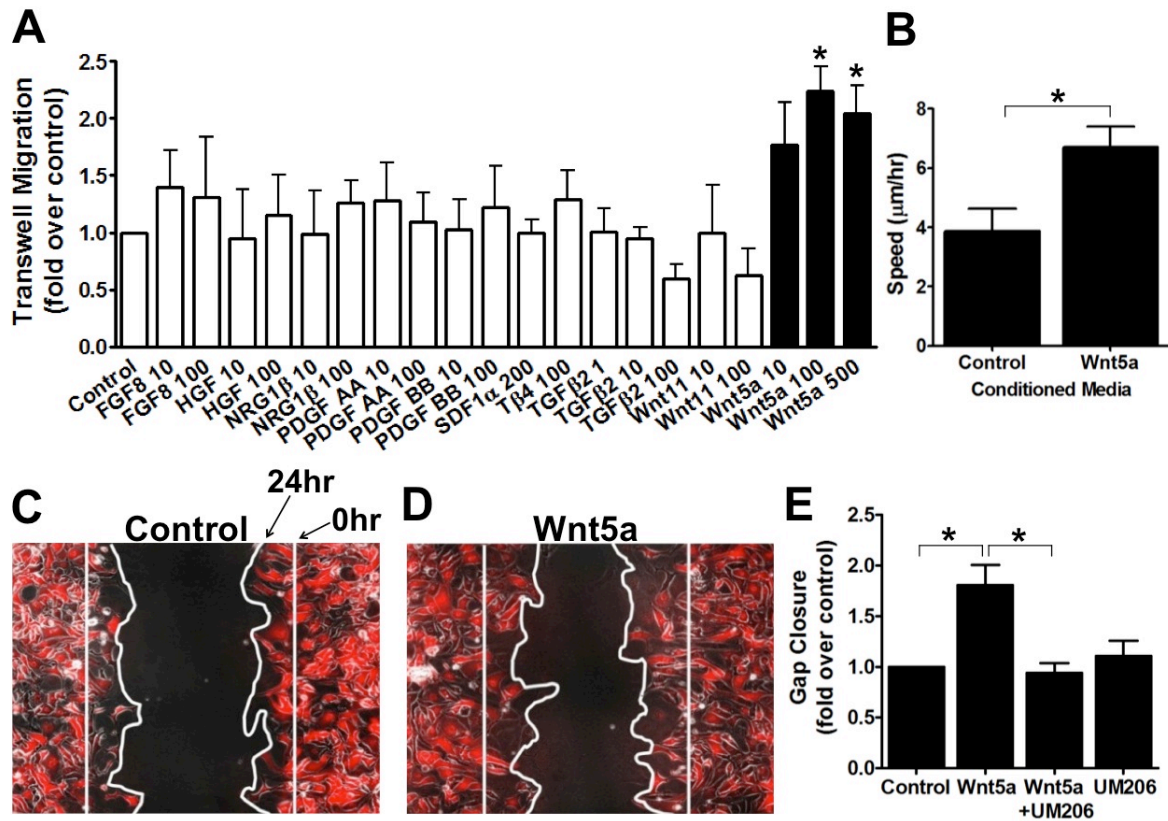


Figure 2.4. Wnt5a is a pro-migratory factor for hESC-CMs. (A): We screened 10 soluble factors for effects on hESC-CM migration in the transwell assay. The only factor showing a significant pro-migratory effect was Wnt5a, which induced a ~two-fold increase in migration at concentrations of 100 and 500 ng/mL. N=4, *p<0.05. (B): During live-cell microscopy of hESC-CMs on unpatterned FN, Wnt5a accelerated random migration by ~two-fold. N=20, *p<0.05. (C-D): Representative images of hESC-CMs in the gap closure assay after 24-hours exposure to control-CM (C) or Wnt5a-CM (D). (E): Wnt5a treated cells migrated to cover ~two-fold more surface area than control cells, a response that was inhibited by UM206 (100nM). *p<0.05, N=4.

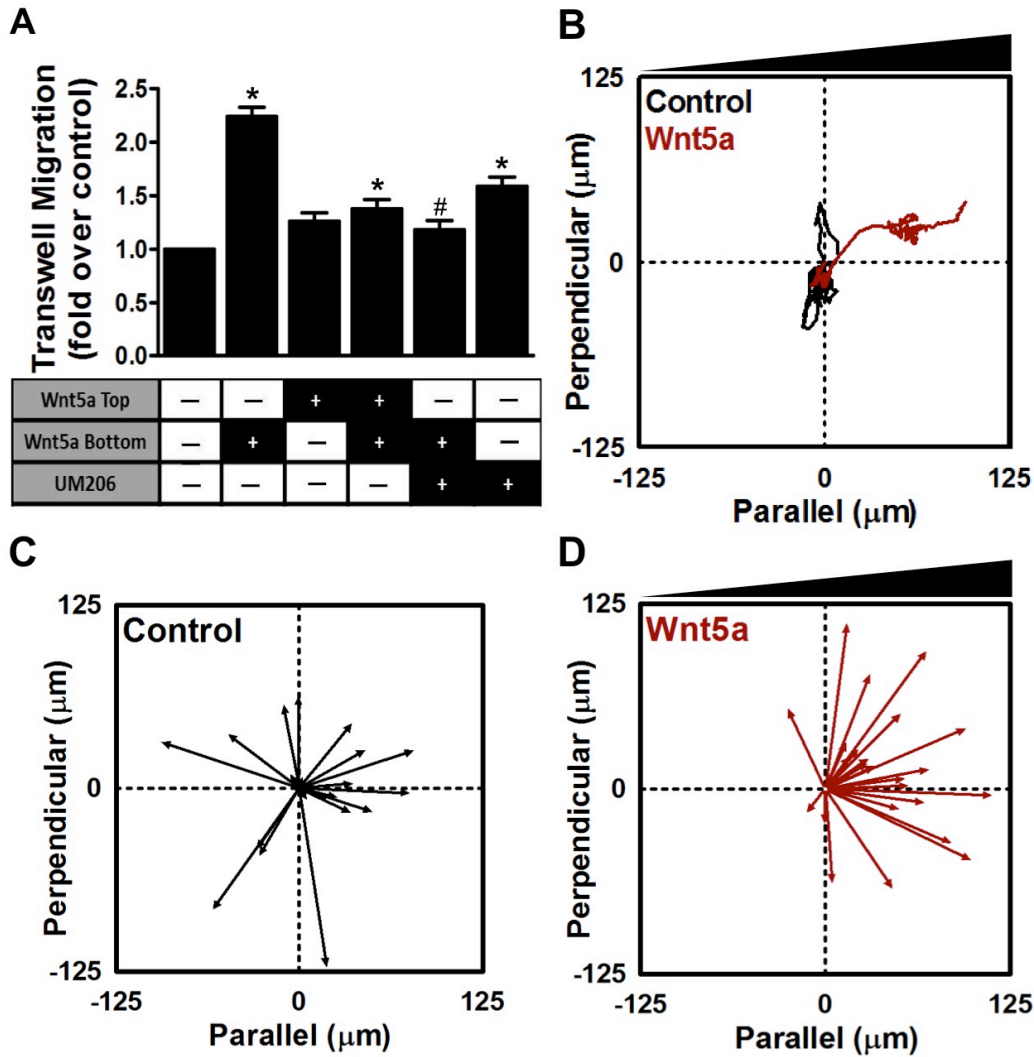


Figure 2.5. Wnt5a is chemotactic for hESC-CMs. (A): Checkerboard assay in which Wnt5a-CM was placed on either the top or bottom of the membrane in the presence or absence of UM206 (100nM). Wnt5a promoted the most migration when placed in the bottom chamber, indicating a chemotactic effect. This response was inhibited by UM206. # Versus Wnt5a Bottom, * Versus Control, N=4, $p < 0.001$. (B): Representative migration paths for hESC-CMs under control conditions (black) and during exposure to a Wnt5a gradient (red). Displacement vectors of hESC-CMs in control-CM (C) and Wnt5a-CM (D) gradients. N=21-24 cells per condition.

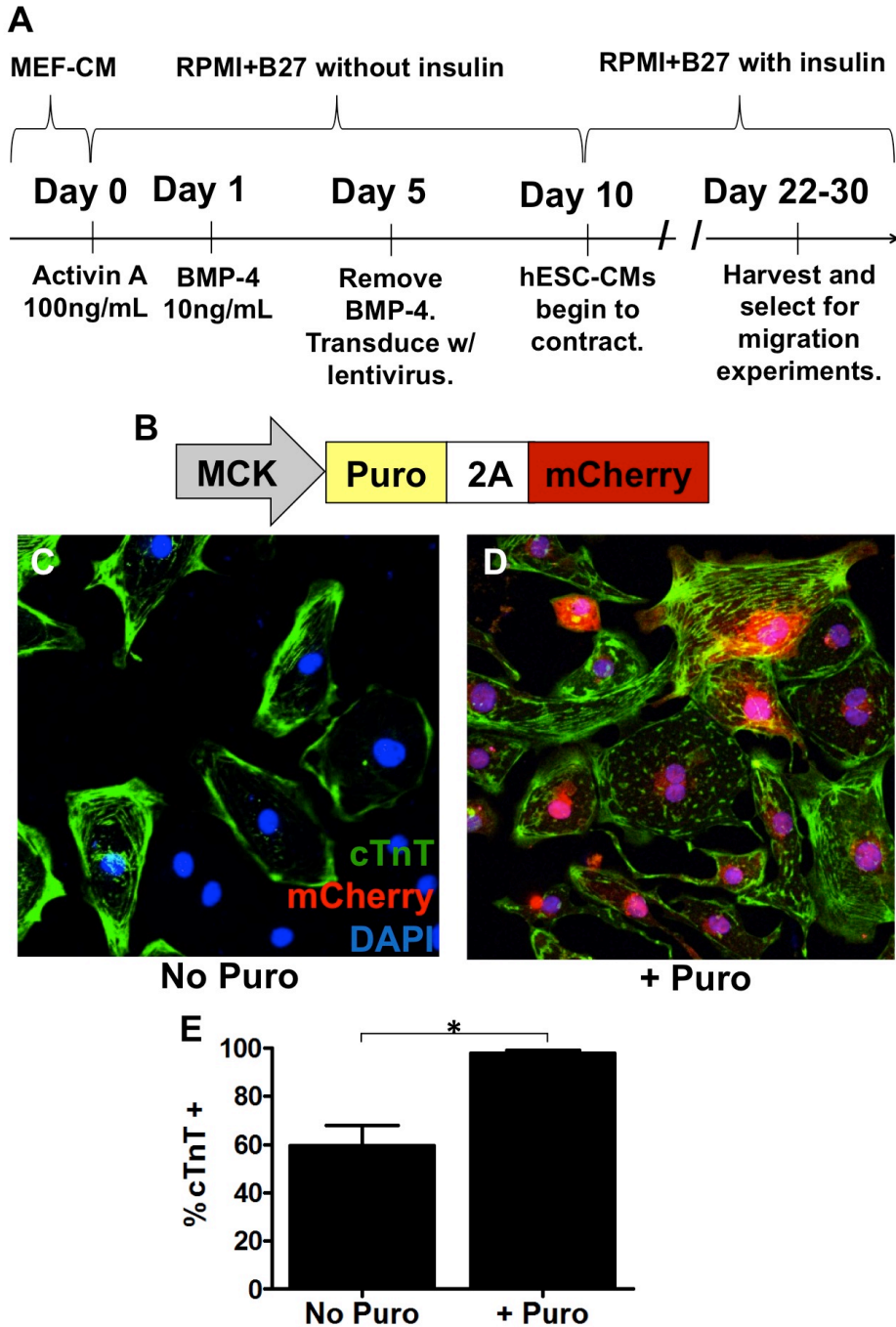


Figure S2.1. Generation and genetic selection of hESC-CMs. (A): Timeline for the directed cardiac differentiation of hESCs and the subsequent genetic selection of hESC-CMs. **(B):** Lentiviral construct in which the muscle creatine kinase (MCK) promoter drives expression of puromycin resistance and the fluorescent reporter, mCherry. Confocal images of transduced hESC-CMs before **(C)** and after **(D)** puromycin selection. Cells were immunostained with antibodies against mCherry (red) and cTnT (green). **(E):** Selection yields a population that is nearly 100% cTnT+. N=4, *p<0.05.

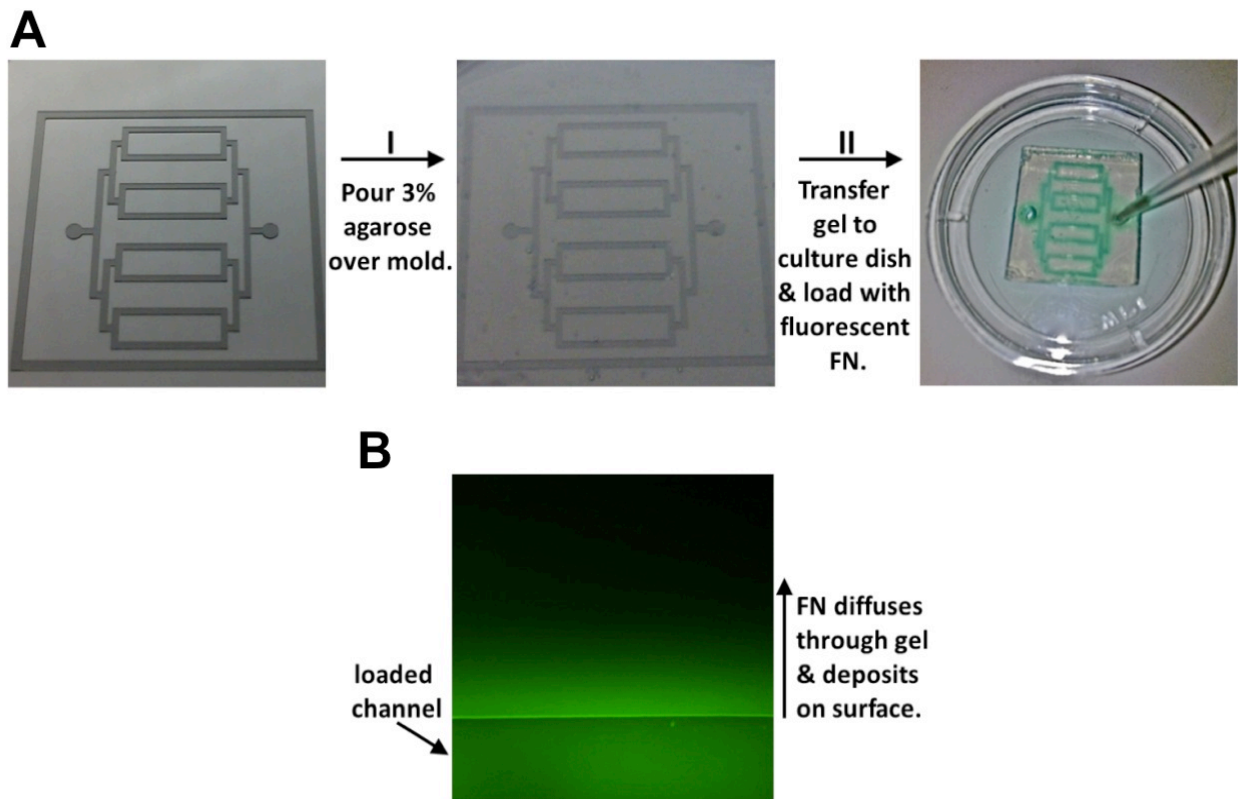


Figure S2.2. Agarose diffusive printing generates surface-bound gradients of FN. (A): To generate these gradients, we poured agarose over the silicon mold and allow it to solidify (**step I**). Next, we transferred the gel to a tissue culture dish and loaded the channels with FN labeled with Oregon-488 (**step II**). The labeled protein then diffused through the gel and deposited on the underlying glass surface. **(B):** View from above of an agarose stamp after dye loading and diffusion into the gel. Note the gradient from the loaded channel (bottom of the field) into the immediately adjacent gel.

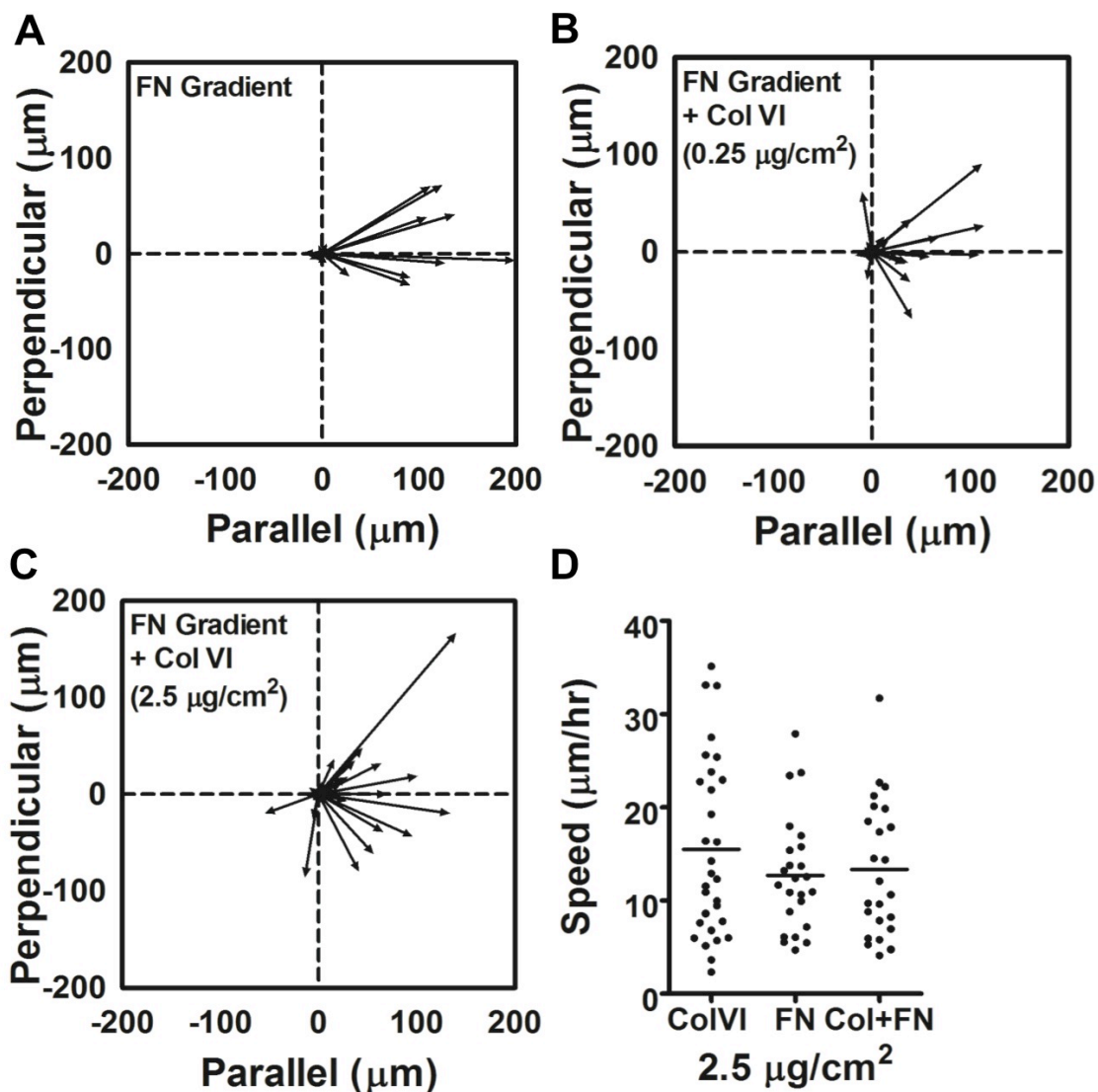


Figure S2.3. Effect of Col VI on the haptotactic response to FN.

(A-C): We used live-cell microscopy to track hESC-CM migration on steep FN gradients both with and without the addition of a uniform concentration of Col VI. Cells on the FN gradient alone (A) tended to migrate further than those on the gradient with Col VI at either 0.25 (B) and $2.5 \mu\text{g}/\text{cm}^2$ (C), although these differences did not reach statistical significance. (D) We also tracked the random migration of hESC-CMs cultured on surfaces coated with a uniform concentration of Col VI alone, FN alone, or Col VI plus FN. Individual cells showed a wide range of migration speeds, and there was no significant difference between conditions.

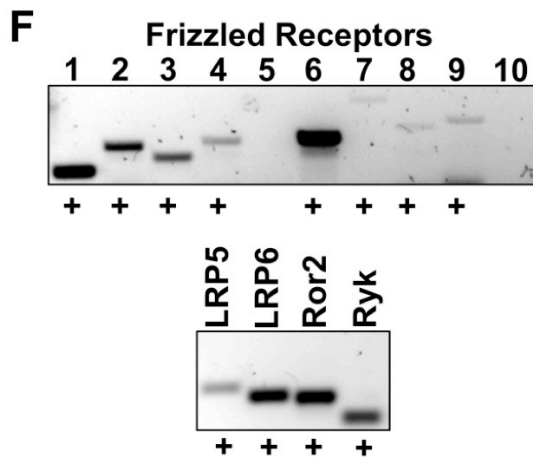
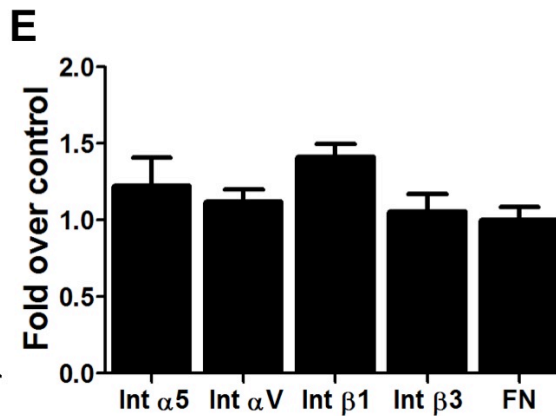
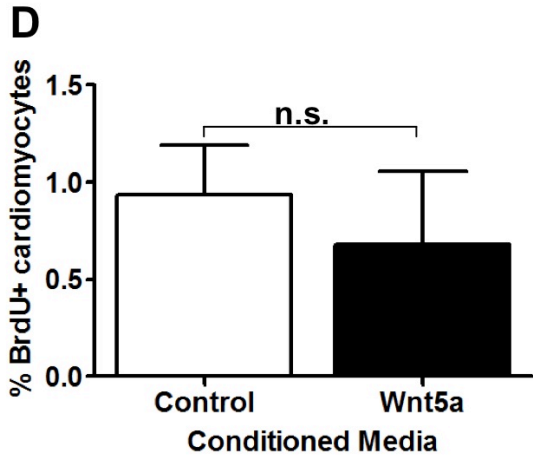
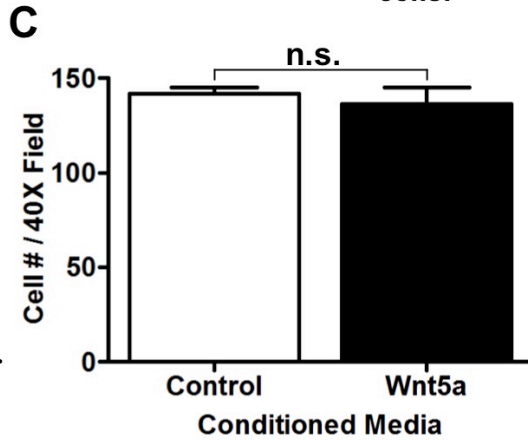
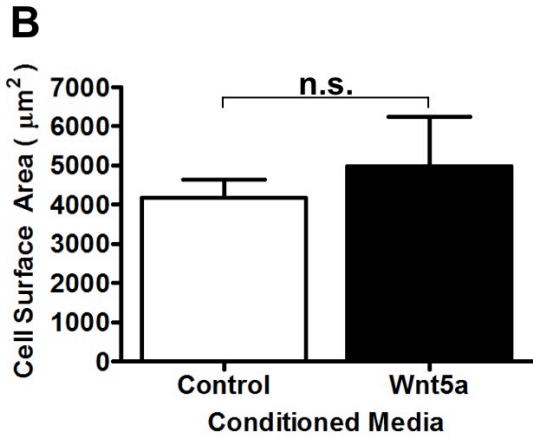
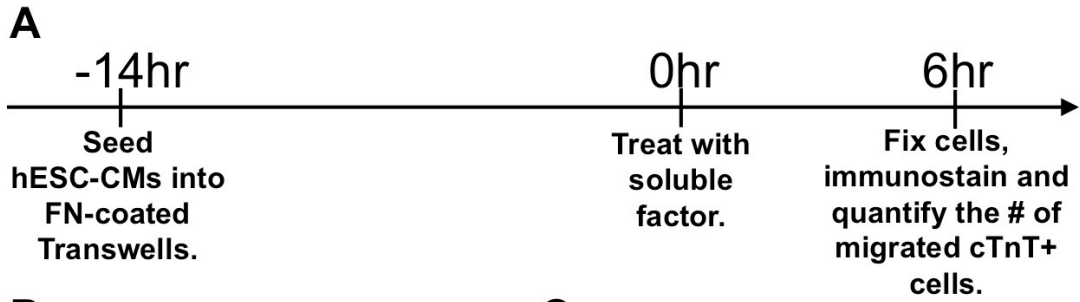


Figure S2.4. Additional studies to characterize the migratory response of hESC-CMs to Wnt5a. (A): Time-course for transwell experiments used to screen Wnt5a and other soluble ligands for effects on hESC-CM migration. In brief, hESC-CMs were allowed to attach to the membrane for 14 hours prior to treatment with the candidate factors. We then placed the candidate factor on the bottom of the transwell and determined the number of cTnT+ hESC-CMs that migrated in the following 6 hours. (B-D): Wnt5a-enhanced gap closure was not accounted for by effects on cell surface area (B), cell retention (C) or proliferation (D). N=4. (E): By qRT-PCR, there was no significant change in the expression of FN or its receptors (integrins $\alpha 5$, αV , $\beta 1$ and $\beta 3$) following 6 hour treatment with Wnt5a. N=3 (F): RT-PCR shows that hESC-CMs express Frizzled (Fzd) receptors 1-4 and 6-9, as well as the Wnt receptors LRP5, LRP6, Ror2 and Ryk.

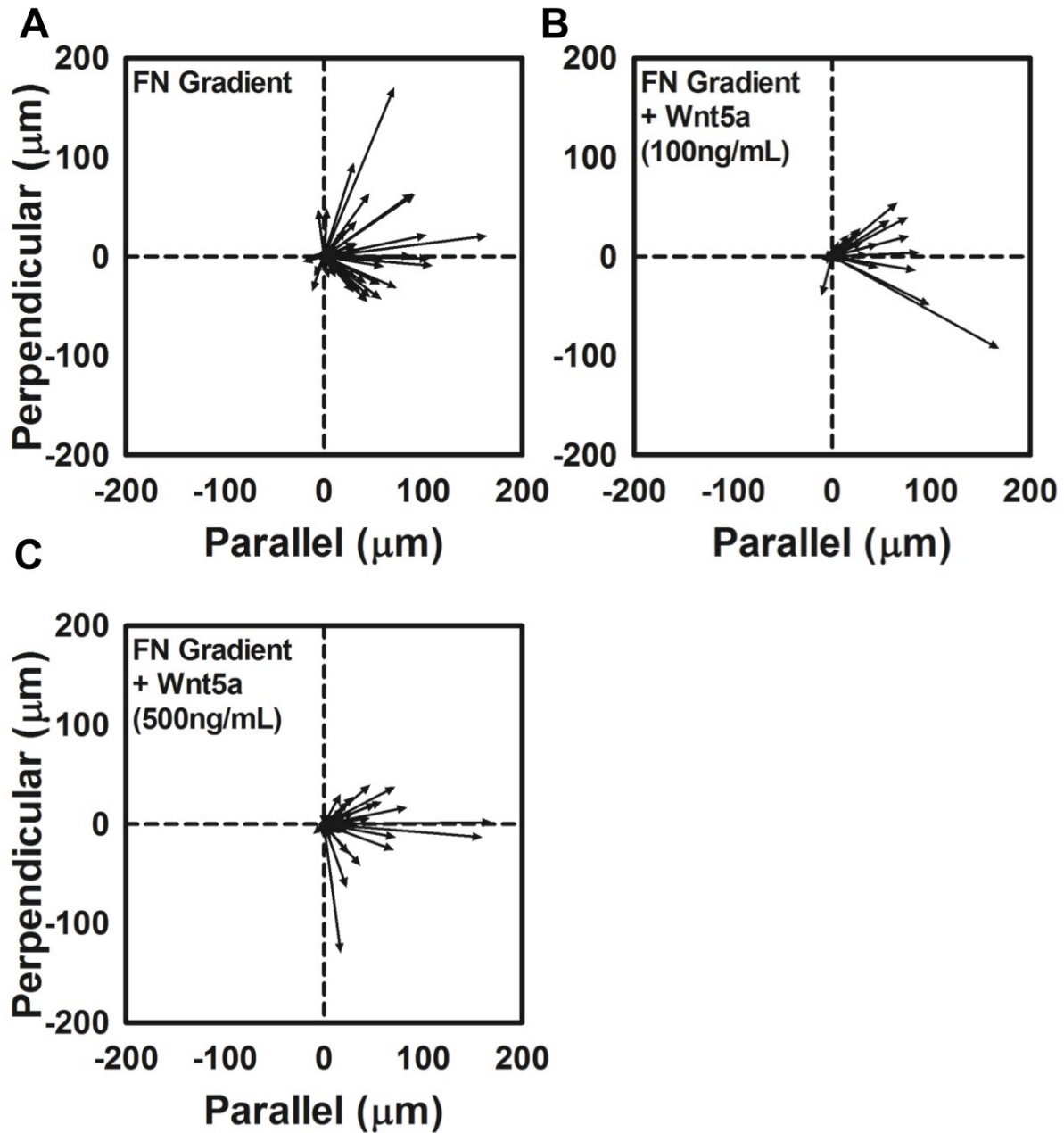


Figure S2.5. Effect of Wnt5a on haptotactic response to FN.

(A-C): We used live-cell microscopy to compare migration on steep FN gradients by control and Wnt5a-stimulated hESC-CMs. There was no statistically significant difference in term of migration vectors relative to the FN gradient between control (A) cells and those with Wnt5a at 100ng/mL (B) or 500ng/mL (C).

ECM Proteins	
Collagen I	Major component of infarct scar[192]
Collagen VI	Component of cardiac jelly and potential player in heart defects of DS patients[108]
Fibronectin	Essential for closure of the embryonic heart tube[86]
Laminin	Cardiomyocyte basement membrane[174]
Vitronectin	Expressed in the endocardial cushion at boundaries with the myocardium[173]
Soluble Factors	
FGF8	Required for addition of SHF myocardium to the OFT[88]
HGF	Enhances skeletal myoblast migration across an endothelial layer[168]
PDGF AA	Enhances skeletal myoblast migration across an endothelial layer[168]
PDGF BB	Enhances skeletal myoblast migration across an endothelial layer[168]
NRG-1	Implicated in directing cardiomyocytes migration during trabeculation[94]
SDF1α	Cardiac progenitor cells migrate toward injured myocardium expressing SDF1 α [169]
TGFβ2	Role in septation and myocardialization[172] Downstream of Wnt11 in heart morphogenesis[123]
Tβ4	Activates integrin-linked kinase and promotes cardiac cell migration[170]
Wnt5a	Required for septation of the outflow tract[122] and ventricular septum[116]
Wnt11	Controls ventricular myocardium development by patterning N-cadherin & β -catenin[97] Role in septation and myocardialization[123]

Table 2.1 Candidate ECM and soluble factors screened in Figures 2.1, 2.2 and 2.4.

Integrin	Sense	Sequence (5' to 3')	Size	Ref
Int α 1	A	ATAAGTGGCCCAGCCAGAG	426	N/A
	S	ACTGCAGCGAAAATCTACCC		
Int α 2	S	CACTCGATTTGGTTCAGCAA	283	[193]
	A	GAACCACTTGTCCAAAGGCA		
Int α 3	S	GCCAGCATTGGTGACATCAA	179	[193]
	A	GAATAGCCGAAGGTGGCCAA		
Int α 4	S	ATGCTGCAAGATTTGGGGAA	265	[193]
	A	GCACCAACTGCTACATCTAC		
Int α 5	S	CCAGGATGGCTACAATGATG	222	[193]
	A	CCCACAATCAGATCAGGATA		
Int α 6	S	CAAGATGGCTACCCAGATAT	210	[193]
	A	CTGAATCTGAGAGGGAACCA		
Int α 7	A	GCTGGTCCACGCCCGCTTCTGTA	241	[192]
	S	GGCCCGGACCCCTGAGTAGTGC		
Int α 10	A	ATCTGGCCTGGCACAGTAAC	201	N/A
	S	TGAACTTCAGACCAGGGGTAG		
Int α 11	A	GTTGGGCTTGACCTCGTAGT	127	N/A
	S	TGACAGTAATGAGCGGGACA		
Int α 11b	S	CTGACTGGCACACAGCTCTA	241	[193]
	A	ATGTCTACGGCACCTCGAAG		
Int α L	S	GAAGAAGTCTCAGAGCTGCA	273	[193]
	A	ATCCCCTTCAAGGTCCTTCA		
Int α M	S	TGTGATGCTGTTCTCTACGG	300	[193]
	A	TCCTACAGTCAGGTCTACCA		
Int α V	S	AGATCTGGACCAGGATGGTT	197	[193]
	A	ATCTGTGGCTCCTTTCATTG		
Int α X	S	GTGCTGTCTACCTGTTTCAC	158	[193]
	A	AGCCAGGTCCACCAGTCCAT		
Int β 1	S	GTTACACGGCTGCTGGTGTT	264	[193]
	A	CTACTGCTGACTTAGGGATC		
Int β 2	S	ACCTGGAGGACAACCTTGTAC	206	[193]
	A	TGAGATGGACCACATTGCTG		
Int β 3	A	TGACGCTAACTGACCAGGTG	232	N/A
	S	CCGTCATTAGGCTGGACAAT		
Int β 4	A	CAGCTCACCAGCGACTACAC	248	N/A
	S	ACACAGCTGTCTGCAGGATG		
Int β 5	A	CCACAGTGTGCGTGGAGATA	168	N/A
	S	TCGGTAGCATCCTCCTTGTT		

Table 2.2 Primers used to amplify integrin transcripts from hESC-CM cDNA.

Wnt Receptor	Sense	Sequence (5' to 3')	Size	Ref
Fz1	A	GTGAGCCGACCAAGGTGTAT	184	[194]
	S	CAGCCGGACAAGAAGATGAT		
Fz2	A	GCGTCTTCTCCGTGCTCTAC	286	[194]
	S	CTGTTGGTGAGGCGAGTGTA		
Fz3	A	TGAGTGTTTCGAAGCTCTATGG	229	[194]
	S	ATCACGCACATGCAGAAAAG		
Fz4	A	AACCTCGGCTACAACGTGAC	303	[194]
	S	GTTGTGGTCGTTCTGTGGTG		
Fz5	A	AACCTCGGCTACAACGTGAC	322	[194]
	S	GTTGTGGTCGTTCTGTGGTGC		
Fz6	A	ATTTTGGTGTCCAAGGCATC	311	[194]
	S	TATTGCAGGCTGTGCTATCG		
Fz7	A	GTGCAGTGTTCTCCCGAACT	544	[194]
	S	GAACGGTAAAGAGCGTCGAG		
Fz8	A	TCTTGTCGCTCACATGGTTC	375	[194]
	S	TGTAGAGCACGGTGAACAGG		
Fz9	A	CGCTGGTCTTCCTACTGCTC	414	[194]
	S	AGAAGACCCCGATCTTGACC		
Fz10	A	GCGGTGAAGACCATCCTG	276	[194]
	S	GCACGGTGTACAGCACAGAG		
LRP5	A	ACCGGAACCACGTACAG	305	[194]
	S	GGGTGGATAGGGGTCTGAGT		
LRP6	A	AGGCACTTACTTCCCTGCAA	274	[194]
	S	GGGCACAGGTTCTGAATCAT		
Ror2	A	GACCCTTTAGGACCCCTTGA	269	N/A
	S	CCAGTGTCTGTCGTGTCCAG		
RYK	A	CGGTCTTGATGCAGAACTTT	203	N/A
	S	CCCCCTGAACAGAAATGTTG		

Table 2.3 Primers used to amplify Wnt receptor transcripts from hESC-CM cDNA.

Chapter 3: Discussion

Above I have shown evidence that FN is haptotactic and Wnt5a is both chemokinetic and chemotactic for hESC-CMs. The limitations of this study and the unanswered questions surrounding hESC-CM migration are discussed below. As stated earlier, the major goal of this study was to gain a better understanding of the factors involved in heart morphogenesis and to identify molecules that could be used to guide hESC-CM migration in infarcted myocardium. The implications of our findings for heart development and cardiac therapy are described in more detail in section 3.2. Next, I will describe future experiments designed to define the role of Wnt5a in the developing outflow tract and to elucidate the mechanism(s) by which this protein drives hESC-CM migration. I will then close by suggesting work to be performed in vitro that will prepare us to test the hypothesis that host-graft integration can be improved by guiding the migration of hESC-CMs in infarcted myocardium.

3.1 Limitations of this Study

Our findings in the present study are well-supported by prior work suggesting that FN and Wnt5a act as guidance cues for early cardiomyocytes in model organisms. However, because we took a candidate molecule approach in this study, we cannot rule out the possibility that other factors (or combinations of factors) might also promote hESC-CM migration. Indeed, a high throughput screen of small molecules to identify additional pro-migratory targets would be valuable. The information gained from such a screen would not only provide more options for guiding hESC-CM migration in vivo, but could lead to the discovery of novel pathways that are important for heart morphogenesis.

Here we deliberately focused on hESC-CMs at a stage of maturation comparable to that used in our prior in vitro and transplantation studies [171, 179], but it is important to note that we have also observed cardiomyocyte motility in cultures after 100-days of in vitro maturation (data not shown). While beyond the scope of the present work, it would be of obvious interest to investigate in the future how motility is affected by parameters including their stage of maturation and electrophysiological phenotype [33, 63, 179].

3.2 Implications of this Work

3.2a hESC-CM migration as a model for human heart morphogenesis

Our findings with hESC-CMs cultured on various ECM substrates are pertinent to cardiac development. In the developing chick heart, FN is expressed in an anterior-to-posterior gradient, which has been implicated in the directed migration of pre-cardiac mesodermal cells anteriorly and to the midline [84]. Subsequent studies in the mouse [85] and zebrafish [86] have confirmed the importance of FN in the formation of the primary heart tube, but its precise role in guiding cellular migration in these models remains unclear. Although we are unaware of any direct evidence of a FN gradient during closure of the human heart tube, our data suggests that this molecule could act as an effective guidance cue for early human cardiomyocytes.

It is also worth noting that we observed the fastest migration speeds (up to 35 $\mu\text{m}/\text{hour}$) with hESC-CMs cultured on collagen VI. We included this ECM molecule in our screens because its gene lies on chromosome 21 and it has been suggested by some as a potential culprit in the congenital heart defects associated with Down Syndrome [108, 195, 196]. Collagen VI has been reported to be overexpressed in the atrioventricular region in trisomy 21 [108], and it has been speculated that this results in aberrant cell migration and cardiac malformation [108, 197].

In future work, it would be of interest to revisit selected experiments from this study using induced pluripotent stem (iPS) cells from normal subjects and patients with congenital heart disease. By comparing the migratory responses of wild type and diseased cardiomyocytes (or wild type cardiomyocytes to the ECM from diseased fibroblasts), we can explore the hypothesis that perturbed cardiomyocyte migration contributes to some instances of structural heart disease [113, 114].

Our finding that Wnt5a is chemoattractive for hESC-CMs is compatible with prior studies of normal and abnormal cardiac development in model organisms. Wnt5a is known to be expressed in the cushion mesenchyme at the time of myocardialization [99, 113, 122], which places this signal at a suitable location to guide the migration of cardiomyocytes into the adjacent cushion to muscularize the outflow tract septum. Transgenic mice lacking Wnt5a [122] or the Wnt receptors Fzd1 or Fzd2 [119] all show defective outflow tract septation. Interestingly, the loss of other components of the non-canonical Wnt signaling pathway, including Ror2, Vangl2 and Dishevelleds 2 or 3, also results in septal defects [113, 116, 120]. When taken collectively with our own findings using human cardiomyocytes, these studies raise the possibility that aberrant Wnt5a signaling and defective cardiomyocyte migration could contribute to dysmorphogenesis in humans. Interestingly, while the best evidence for Wnt5a-induced cardiomyocyte migration in non-human models comes from studies of outflow tract development [99, 113, 116, 119, 120, 122, 177, 198], nearly all hESC-CMs showed Wnt5a responsiveness in our live cell-imaging studies. Our hESC-CM preparations have been previously shown to include multiple cardiac subtypes [179], implying that Wnt5a-mediated migration is not limited to a minor subset of hESC-CMs.

3.2b Guided migration to enhance electrical coupling

In addition to being a model for human heart development, hESC-CMs have attracted significant interest as a potential cell source for remuscularizing infarcted heart tissue. In recent work, our lab found that hESC-CMs can couple with host myocardium following transplantation into infarcted myocardium, but many hESC-CM implants remain electrically isolated by intervening scar tissue [171]. The present study suggests a number of novel strategies for improving their electromechanical integration. For example, by providing a suitable chemokinetic signal (e.g. Wnt5a), one might stimulate the random migration of hESC-CMs in vivo and increase the likelihood of host-graft or graft-graft contact. Support for this possibility comes from our experiments in the gap closure assay, in which Wnt5a-stimulated hESC-CMs covered ~250 μm distance within a 24-hour period. It might also be possible to harness the chemoattractant properties of Wnt5a by injecting Wnt5a-eluting controlled release microspheres [199, 200] into the infarct border zone (perhaps with guidance by electroanatomic mapping). If this intervention resulted in an appropriately inductive Wnt5a gradient, hESC-CM grafts isolated in scar tissue might be drawn toward viable host muscle and/or better-coupled graft implants in the border zone. The hydrophobicity and special packaging needs of Wnt5a will surely be a consideration when we explore this molecule for these purposes. Perhaps a small molecule agonist or peptide mimetic will be required to achieve the desired outcome. Additionally, migration might be also facilitated by the delivery of hESC-CMs within FN or collagen VI-based hydrogels [201, 202] as opposed to the laminin-based matrigel that is currently used.

Of course, any of the preceding strategies would have to take into account the biological activity and the patterns of endogenous expression of the factor(s) employed. For example,

endogenous Wnt5a has been implicated in myofibroblast differentiation and migration during early infarct repair [187]. FN and collagen VI expression are known to be up-regulated in the early post-infarct heart, where they are thought to help facilitate inflammation and ventricular remodeling [138, 203]. FN signaling may also promote undesirable effects such as cardiac fibrosis [204] or cardiomyocyte hypertrophy [205]. We may be able to avoid such off-target effects by limiting delivery of the cells and the exogenous factor to the already-established infarct scar or by using appropriate synthetic biomaterials (e.g. hydrogels with incorporated FN functional domains [201]).

3.3 Future Studies

3.3a Is Wnt5a Pro-Migratory for Cardiomyocytes in the Developing OFT Septum?

Here we've shown that Wnt5a is pro-migratory for cardiomyocytes derived from hESCs, but in the future one could test the hypothesis that Wnt5a also has pro-migratory effect on cardiomyocytes of the developing OFT septum. As stated in section 1.2d, there is substantial evidence demonstrating that non-canonical Wnt signaling plays an important role in OFT septation and that cardiomyocyte migration is necessary for this process (**Table 1.3**). However, until now no studies have made the direct connection between non-canonical Wnts and cardiomyocyte migration. Therefore, it is unclear if Wnts are affecting migration, proliferation or differentiation or if Wnts are acting indirectly through another cell type (e.g. cardiac neural crest cells). The Wessels and Moorman groups showed that MF20 positive myocytes from chick and mouse OFT explants were able to invade a collagen gel and form myocardial networks [115, 206]. In this study they found that myocardium that was explanted at a time prior to the onset of myocardialization of the OFT septum was incapable of invading the collagen gel but if

these early explants were cultured with media conditioned by later, myocardializing tissue, the invasive capacity was restored. These findings indicate that there is a soluble factor responsible for inducing this process. Using this approach, one could test the hypothesis that Wnt5a is the responsible factor and perhaps establish a definitive pro-migratory role for Wnt5a in this morphogenic process.

3.3b Elucidating the Mechanism of Wnt5a Mediated Migration

In this study we demonstrated that the Frizzled 1/2 antagonist UM206, blocks both the chemokinetic and chemotactic effects of Wnt5a in hESC-CMs, but future experiments using shRNA will be required to confirm the role of Frizzled 2 and to determine if Ror2 is also involved in these responses. The mechanism of Wnt5a-mediated migration in hESC-CMs downstream of the receptor(s) also remains to be elucidated. As mentioned earlier, the calcium and PCP pathways both signal through Frizzleds and Ror2 and they likely have some degree of overlap. To determine which is active in hESC-CMs, one could inhibit the activity of the kinases that distinguish these two pathways, PKC and JNK [153], and monitor the migratory response and phosphorylation state of their downstream targets, focal adhesion kinase [207] and paxillin [208] respectively (See **Figure 3.1** for overview).

3.3c In Vitro Modeling of In Vivo Studies

There are some questions that remain to be answered in vitro before the hypothesis that guided hESC-CM migration will improve electrical coupling in vivo can be tested. For example, all of our current experiments were performed in 2D so it is yet unknown whether hESC-CMs have the ability to invade dense collagenous tissue or if the cells will respond to

Wnt5a in a 3D system. As a proof of concept experiment, future scientists in the Laflamme lab will model the ability of Wnt5a to drive hESC-CM migration through scar tissue by using a 3D collagen invasion assay. This in vitro modeling may reveal that hESC-CMs are incapable of migrating an effective distance in 3D, even when stimulated with a chemoattractive molecule. One explanation for this would be the lack of expression or activation of enzymes necessary to degrade the surrounding matrix. While Wnt5a up-regulates the expression of MMPs in cancer cells [142, 186, 209, 210], it does not alter the expression of MMPs in hESC-CMs cultured on a fibronectin-coated surface (**Figure 3.2**). The effect of Wnt5a on MMP expression or activation in hESC-CMs in a collagen matrix is still unknown. If the lack of activity is limiting their ability to invade, one could consider over-expressing a membrane bound protease such as MT1-MMP in hESC-CMs or co-injecting these cells into infarcted myocardium with a second, more invasive cell type.

Additional preliminary work to be completed in vitro includes the design of a controlled release system that is capable of generating a bioactive gradient of Wnt5a in vivo. Various microsphere materials (agarose, heparin, gelatin, etc), should be compared while considering parameters such as loading concentration, release profile and steepness and stability of the gradient. The optimal parameters will be defined by testing the effectiveness of the system in the collagen invasion assay described above.

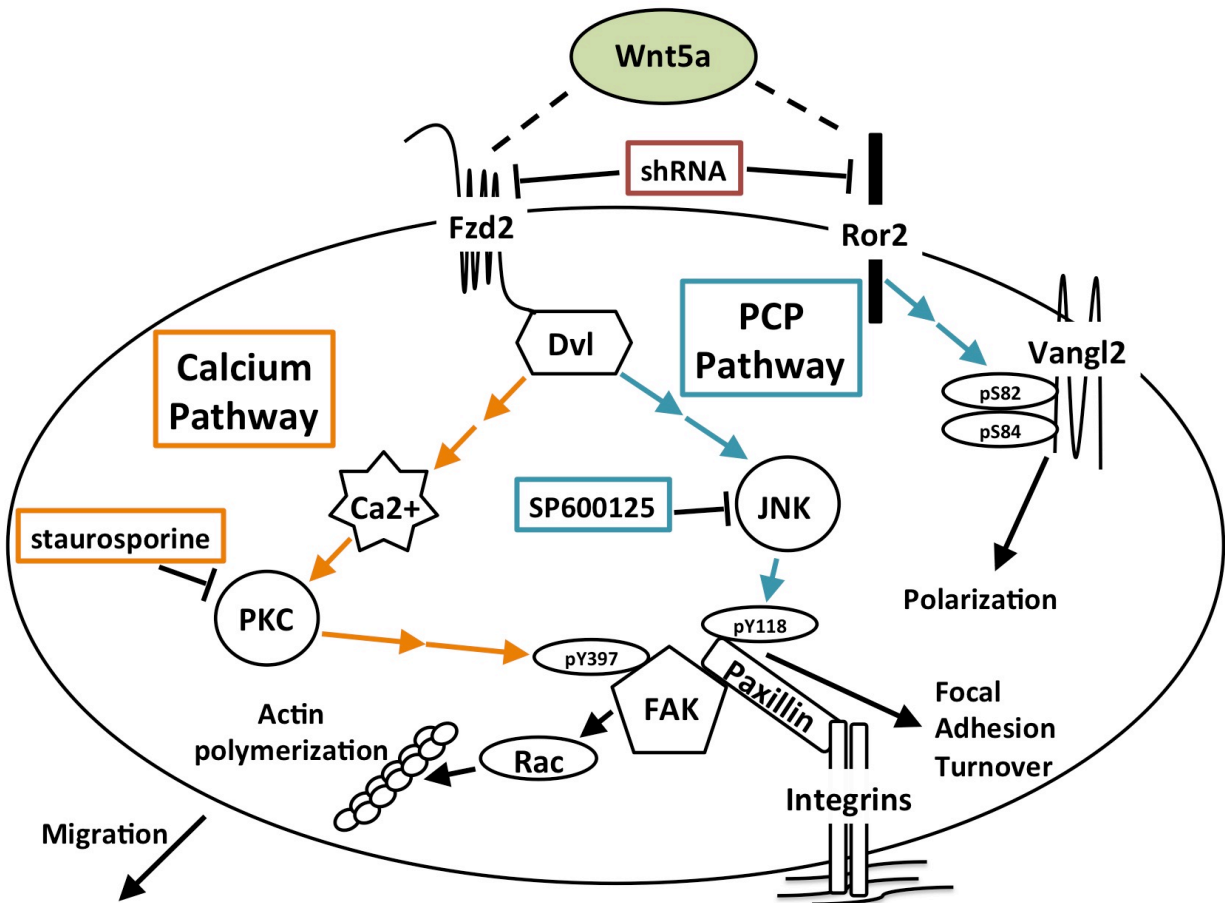


Figure 3.1 Methods for determining the signaling mechanism(s) responsible for Wnt5a induced migration. shRNA will be used to determine if Fzd2 and/or Ror2 are required for Wn5a mediated migration. Dvl acts downstream of Frizzleds to regulate both the calcium (orange) and PCP (blue) pathways. Pharmacologic inhibitors of PKC (staurosporine) and JNK (SP600125) will be employed to determine which of these pathways is active in hESC-CMs.

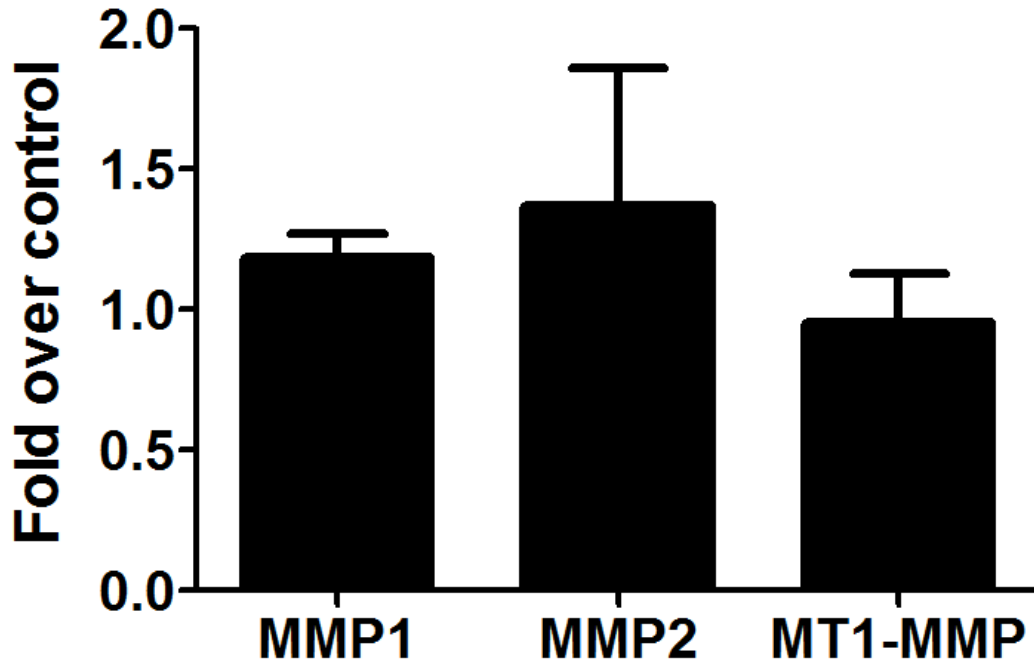


Figure 3.2 Wnt5a does not alter expression of MMPs in hESC-CMs. hESC-CMs cultured on fibronectin coated plates were treated with Wnt5a.CM for 6 hours. Expression levels of MMP1, MMP2 and MT1-MMP were quantified relative to control using qRT-PCR. Note, MMP9 and MMP13 transcripts were not detected in these cells. N=4.

Acknowledgements

To be honest, I have been dreading writing my acknowledgements section for a while. Not because I don't have anything to be thankful for, but because it means I am saying goodbye. I have spent 1/6 of my life in the Pathology Department and over this time, the Laflamme Lab has been my home. There were certainly many moments of exhaustion, confusion and frustration, but in retrospect, those memories are overshadowed by feelings of inspiration, clarity and triumph. Late nights spent in the dark Garvey Imaging Core¹ were followed by sunny days in tissue culture where I would hear Wei-Zhong humming a tune, Ben making an off-the-wall joke and Jon citing the virtues of his favorite super hero. And of course Willi was always there with a smile, eager to count his 3102nd transwell. This experience would not have been the same without Scott and Jay. Over the last several years they've become not just lab-mates that I could bounce ideas off of, but friends who were always there to commiserate and more often, celebrate. Now, as the 3 of us retire together, we pass the torch to Dominic to keep the "Flamme" burning...

...which brings me to Mike. Of course the Laflamme Lab would not be what it is if it weren't for him. Mike brings a special kind of patience, creativity and passion for science that creates the unique environment that we love. He not only holds us to a high standard, but inspires us by setting an example of what it takes to be an accomplished scientist and an effective leader.

I also have many people to thank out side of the lab. Last winter I had the rare opportunity to explore Japan when Yuji Shiba, our former post-doc, invited me to visit his new

¹ Ron Seifert is a saint who tolerated me in spite of my 90GB files and who can solve every imaginable problem.

lab and share my research with his colleagues. They treated me like royalty and even made me eat horse. Steve Berard has never missed an opportunity to share an encouraging word or provide comic relief when it was needed. Sarah Fernandes, my fellow SLUGs co-chair was not only a blast to work with but was always ready to take on adventure, be it a homemade water slide or a circus trapeze.

I would also like to acknowledge my West Seattle family. Julie, my kettle-sister who was kind enough to drop by with surprise teriyaki or Thai food when I was in the depths of writing and could barely find time to shower. Zach and Roo, my coaches who keep me challenged outside of the lab and provided a sanctuary where I can grunt and curse and throw heavy things so that when I'm in the lab, I can act civilized. I can't forget my cats (the Buds and the Gher), who in spite of giving me Cat Scratch Fever and insisting on laying on my keyboard, have been welcome company through many late nights. Of course Paul has been behind me the entire time acting as my co-pilot, sugar daddy and cheerleader. Paul refuses to settle for the ordinary and sees the world with the eyes of an explorer. I can't wait to take this next step in my life with him by my side.

Finally I would like to thank my committee for their wisdom and guidance over the years, particularly Mike, Dan and Elaine who volunteered to read this beast. I am also very grateful to the Cardiovascular Pathology Training Grant and Steve Schwartz not only for keeping me funded, but for encouraging me to step outside my comfort zone and look at my research in unique ways.

References

1. Moyes, K.W., et al., *Human Embryonic Stem Cell-Derived Cardiomyocytes Migrate in Response to Gradients of Fibronectin and Wnt5a*. *Stem Cells Dev*, 2013.
2. Caspi, O., et al., *Transplantation of human embryonic stem cell-derived cardiomyocytes improves myocardial performance in infarcted rat hearts*. *J Am Coll Cardiol*, 2007. **50**(19): p. 1884-93.
3. Laflamme, M.A., et al., *Cardiomyocytes derived from human embryonic stem cells in pro-survival factors enhance function of infarcted rat hearts*. *Nat Biotechnol*, 2007. **25**(9): p. 1015-24.
4. van Laake, L.W., et al., *Human embryonic stem cell-derived cardiomyocytes survive and mature in the mouse heart and transiently improve function after myocardial infarction*. *Stem Cell Res*, 2007. **1**(1): p. 9-24.
5. Shiba, Y., et al., *Human ES-cell-derived cardiomyocytes electrically couple and suppress arrhythmias in injured hearts*. *Nature*, 2012. **489**(7415): p. 322-5.
6. Thomson, J.A. and V.S. Marshall, *Primate embryonic stem cells*. *Curr Top Dev Biol*, 1998. **38**: p. 133-65.
7. Thomson, J.A., et al., *Embryonic stem cell lines derived from human blastocysts*. *Science*, 1998. **282**(5391): p. 1145-7.
8. Ling, V. and S. Neben, *In vitro differentiation of embryonic stem cells: immunophenotypic analysis of cultured embryoid bodies*. *J Cell Physiol*, 1997. **171**(1): p. 104-15.
9. Kim, J., et al., *An extended transcriptional network for pluripotency of embryonic stem cells*. *Cell*, 2008. **132**(6): p. 1049-61.
10. Sharma, H.W., et al., *Differentiation of immortal cells inhibits telomerase activity*. *Proc Natl Acad Sci U S A*, 1995. **92**(26): p. 12343-6.
11. Xu, C., et al., *Feeder-free growth of undifferentiated human embryonic stem cells*. *Nat Biotechnol*, 2001. **19**(10): p. 971-4.
12. Inzunza, J., et al., *Derivation of human embryonic stem cell lines in serum replacement medium using postnatal human fibroblasts as feeder cells*. *Stem Cells*, 2005. **23**(4): p. 544-9.
13. Yoo, S.J., et al., *Efficient culture system for human embryonic stem cells using autologous human embryonic stem cell-derived feeder cells*. *Exp Mol Med*, 2005. **37**(5): p. 399-407.
14. Xu, C., et al., *Immortalized fibroblast-like cells derived from human embryonic stem cells support undifferentiated cell growth*. *Stem Cells*, 2004. **22**(6): p. 972-80.
15. Li, Y., et al., *Expansion of human embryonic stem cells in defined serum-free medium devoid of animal-derived products*. *Biotechnol Bioeng*, 2005. **91**(6): p. 688-98.
16. Lu, J., et al., *Defined culture conditions of human embryonic stem cells*. *Proc Natl Acad Sci U S A*, 2006. **103**(15): p. 5688-93.
17. Ludwig, T.E., et al., *Derivation of human embryonic stem cells in defined conditions*. *Nat Biotechnol*, 2006. **24**(2): p. 185-7.
18. Xu, C., et al., *Basic fibroblast growth factor supports undifferentiated human embryonic stem cell growth without conditioned medium*. *Stem Cells*, 2005. **23**(3): p. 315-23.

19. Bendall, S.C., et al., *IGF and FGF cooperatively establish the regulatory stem cell niche of pluripotent human cells in vitro*. *Nature*, 2007. **448**(7157): p. 1015-21.
20. Levenstein, M.E., et al., *Basic fibroblast growth factor support of human embryonic stem cell self-renewal*. *Stem Cells*, 2006. **24**(3): p. 568-74.
21. Xu, R.-H., et al., *Basic FGF and suppression of BMP signaling sustain undifferentiated proliferation of human ES cells*. *Nature Methods*, 2005. **3**: p. 185-90.
22. Ware, C.B., et al., *Histone deacetylase inhibition elicits an evolutionarily conserved self-renewal program in embryonic stem cells*. *Cell Stem Cell*, 2009. **4**(4): p. 359-69.
23. Desbordes, S.C., et al., *High-throughput screening assay for the identification of compounds regulating self-renewal and differentiation in human embryonic stem cells*. *Cell Stem Cell*, 2008. **2**(6): p. 602-12.
24. Miyabayashi, T., et al., *Wnt/beta-catenin/CBP signaling maintains long-term murine embryonic stem cell pluripotency*. *Proc Natl Acad Sci U S A*, 2007. **104**(13): p. 5668-73.
25. Prowse, A.B., et al., *Identification of potential pluripotency determinants for human embryonic stem cells following proteomic analysis of human and mouse fibroblast conditioned media*. *J Proteome Res*, 2007. **6**(9): p. 3796-807.
26. Chin, A.C., et al., *Identification of proteins from feeder conditioned medium that support human embryonic stem cells*. *J Biotechnol*, 2007. **130**(3): p. 320-8.
27. Doetschman, T.C., et al., *The in vitro development of blastocyst-derived embryonic stem cell lines: formation of visceral yolk sac, blood islands and myocardium*. *J Embryol Exp Morphol*, 1985. **87**: p. 27-45.
28. Robbins, J., et al., *Mouse embryonic stem cells express the cardiac myosin heavy chain genes during development in vitro*. *J Biol Chem*, 1990. **265**(20): p. 11905-9.
29. Kehat, I., et al., *Human embryonic stem cells can differentiate into myocytes with structural and functional properties of cardiomyocytes*. *J Clin Invest*, 2001. **108**(3): p. 407-14.
30. Laflamme, M.A., et al., *Formation of human myocardium in the rat heart from human embryonic stem cells*. *Am J Pathol*, 2005. **167**(3): p. 663-71.
31. Kita-Matsuo, H., et al., *Lentiviral vectors and protocols for creation of stable hESC lines for fluorescent tracking and drug resistance selection of cardiomyocytes*. *PLoS ONE*, 2009. **4**(4): p. e5046.
32. Beltrami, C.A., et al., *Structural basis of end-stage failure in ischemic cardiomyopathy in humans*. *Circulation*, 1994. **89**(1): p. 151-63.
33. Mummery, C., et al., *Differentiation of human embryonic stem cells to cardiomyocytes: role of coculture with visceral endoderm-like cells*. *Circulation*, 2003. **107**(21): p. 2733-40.
34. Fullilove, S.L., *Heart induction: distribution of active factors in newt endoderm*. *J Exp Zool*, 1970. **175**(3): p. 323-6.
35. Schultheiss, T.M., S. Xydas, and A.B. Lassar, *Induction of avian cardiac myogenesis by anterior endoderm*. *Development*, 1995. **121**(12): p. 4203-14.
36. Sugi, Y. and J. Lough, *Anterior endoderm is a specific effector of terminal cardiac myocyte differentiation of cells from the embryonic heart forming region*. *Dev Dyn*, 1994. **200**(2): p. 155-62.

37. Passier, R., et al., *Increased cardiomyocyte differentiation from human embryonic stem cells in serum-free cultures*. *Stem Cells*, 2005. **23**(6): p. 772-80.
38. Freund, C., et al., *Insulin redirects differentiation from cardiogenic mesoderm and endoderm to neuroectoderm in differentiating human embryonic stem cells*. *Stem Cells*, 2008. **26**(3): p. 724-33.
39. Graichen, R., et al., *Enhanced cardiomyogenesis of human embryonic stem cells by a small molecular inhibitor of p38 MAPK*. *Differentiation*, 2008. **76**(4): p. 357-70.
40. Yatskievych, T.A., A.N. Ladd, and P.B. Antin, *Induction of cardiac myogenesis in avian pregastrula epiblast: the role of the hypoblast and activin*. *Development*, 1997. **124**(13): p. 2561-70.
41. Conlon, F.L., et al., *A primary requirement for nodal in the formation and maintenance of the primitive streak in the mouse*. *Development*, 1994. **120**(7): p. 1919-28.
42. Smith, J.C., et al., *Identification of a potent Xenopus mesoderm-inducing factor as a homologue of activin A*. *Nature*, 1990. **345**(6277): p. 729-31.
43. D'Amour, K.A., et al., *Efficient differentiation of human embryonic stem cells to definitive endoderm*. *Nat Biotechnol*, 2005. **23**(12): p. 1534-41.
44. Vallier, L., D. Reynolds, and R.A. Pedersen, *Nodal inhibits differentiation of human embryonic stem cells along the neuroectodermal default pathway*. *Dev Biol*, 2004. **275**(2): p. 403-21.
45. Vallier, L., et al., *Early cell fate decisions of human embryonic stem cells and mouse epiblast stem cells are controlled by the same signalling pathways*. *PLoS ONE*, 2009. **4**(6): p. e6082.
46. Golob, J.L., et al., *Chromatin remodeling during mouse and human embryonic stem cell differentiation*. *Dev Dyn*, 2008. **237**(5): p. 1389-98.
47. Tada, S., et al., *Characterization of mesendoderm: a diverging point of the definitive endoderm and mesoderm in embryonic stem cell differentiation culture*. *Development*, 2005. **132**(19): p. 4363-74.
48. Schultheiss, T.M., J.B. Burch, and A.B. Lassar, *A role for bone morphogenetic proteins in the induction of cardiac myogenesis*. *Genes Dev*, 1997. **11**(4): p. 451-62.
49. Ladd, A.N., T.A. Yatskievych, and P.B. Antin, *Regulation of avian cardiac myogenesis by activin/TGFbeta and bone morphogenetic proteins*. *Dev Biol*, 1998. **204**(2): p. 407-19.
50. Zhu, W.Z., et al., *Human embryonic stem cells and cardiac repair*. *Transplant Rev (Orlando)*, 2009. **23**(1): p. 53-68.
51. McLean, A.B., et al., *Activin efficiently specifies definitive endoderm from human embryonic stem cells only when phosphatidylinositol 3-kinase signaling is suppressed*. *Stem Cells*, 2007. **25**(1): p. 29-38.
52. Lian, X., et al., *Insulin inhibits cardiac mesoderm, not mesendoderm, formation during cardiac differentiation of human pluripotent stem cells and modulation of canonical Wnt signaling can rescue this inhibition*. *Stem Cells*, 2013. **31**(3): p. 447-57.
53. Naito, A.T., et al., *Developmental stage-specific biphasic roles of Wnt/beta-catenin signaling in cardiomyogenesis and hematopoiesis*. *Proc Natl Acad Sci U S A*, 2006. **103**(52): p. 19812-7.

54. Ueno, S., et al., *Biphasic role for Wnt/beta-catenin signaling in cardiac specification in zebrafish and embryonic stem cells*. Proc Natl Acad Sci U S A, 2007. **104**(23): p. 9685-90.
55. Yang, L., et al., *Human cardiovascular progenitor cells develop from a KDR+ embryonic-stem-cell-derived population*. Nature, 2008. **453**(7194): p. 524-8.
56. Yang, L., et al., *Human cardiovascular progenitor cells develop from a KDR(+) embryonic-stem-cell-derived population*. Nature, 2008.
57. Zhang, J., et al., *Extracellular matrix promotes highly efficient cardiac differentiation of human pluripotent stem cells: the matrix sandwich method*. Circ Res, 2012. **111**(9): p. 1125-36.
58. Lian, X., et al., *Directed cardiomyocyte differentiation from human pluripotent stem cells by modulating Wnt/beta-catenin signaling under fully defined conditions*. Nat Protoc, 2013. **8**(1): p. 162-75.
59. Zhu, W.Z., L.F. Santana, and M.A. Laflamme, *Local control of excitation-contraction coupling in human embryonic stem cell-derived cardiomyocytes*. PLoS ONE, 2009. **4**(4): p. e5407.
60. McDevitt, T.C., M.A. Laflamme, and C.E. Murry, *Proliferation of cardiomyocytes derived from human embryonic stem cells is mediated via the IGF/PI 3-kinase/Akt signaling pathway*. J Mol Cell Cardiol, 2005. **39**(6): p. 865-73.
61. Cui, L., et al., *Structural differentiation, proliferation, and association of human embryonic stem cell-derived cardiomyocytes in vitro and in their extracardiac tissues*. J Struct Biol, 2007. **158**(3): p. 307-17.
62. Xu, C., et al., *Characterization and enrichment of cardiomyocytes derived from human embryonic stem cells*. Circ Res, 2002. **91**(6): p. 501-8.
63. He, J.Q., et al., *Human embryonic stem cells develop into multiple types of cardiac myocytes: action potential characterization*. Circ Res, 2003. **93**(1): p. 32-9.
64. Lev, S., I. Kehat, and L. Gepstein, *Differentiation pathways in human embryonic stem cell-derived cardiomyocytes*. Ann N Y Acad Sci, 2005. **1047**: p. 50-65.
65. Xu, C., et al., *Human embryonic stem cell-derived cardiomyocytes can be maintained in defined medium without serum*. Stem Cells Dev, 2006. **15**(6): p. 931-41.
66. Dai, W., et al., *Survival and maturation of human embryonic stem cell-derived cardiomyocytes in rat hearts*. J Mol Cell Cardiol, 2007. **43**(4): p. 504-16.
67. Kehat, I., et al., *High-resolution electrophysiological assessment of human embryonic stem cell-derived cardiomyocytes: a novel in vitro model for the study of conduction*. Circ Res, 2002. **91**(8): p. 659-61.
68. Kehat, I., et al., *Electromechanical integration of cardiomyocytes derived from human embryonic stem cells*. Nat Biotechnol, 2004. **22**(10): p. 1282-9.
69. Xue, T., et al., *Functional integration of electrically active cardiac derivatives from genetically engineered human embryonic stem cells with quiescent recipient ventricular cardiomyocytes: insights into the development of cell-based pacemakers*. Circulation, 2005. **111**(1): p. 11-20.
70. Kehat, I., et al., *High-resolution electrophysiological assessment of human embryonic stem cell-derived cardiomyocytes: a novel in vitro model for the study of conduction*. Circulation Research, 2002. **91**(8): p. 659-61.

71. Gepstein, L., et al., *In vivo assessment of the electrophysiological integration and arrhythmogenic risk of myocardial cell transplantation strategies*. *Stem Cells*, 2010. **28**(12): p. 2151-61.
72. Zimmermann, W.H., et al., *Engineered heart tissue grafts improve systolic and diastolic function in infarcted rat hearts*. *Nat Med*, 2006. **12**(4): p. 452-8.
73. Dvir, T., et al., *Prevascularization of cardiac patch on the omentum improves its therapeutic outcome*. *Proc Natl Acad Sci U S A*, 2009. **106**(35): p. 14990-5.
74. Baklanov, D.V., et al., *Comparison of transendocardial and retrograde coronary venous intramyocardial catheter delivery systems in healthy and infarcted pigs*. *Catheter Cardiovasc Interv*, 2006. **68**(3): p. 416-23.
75. Hoshino, K., et al., *Three catheter-based strategies for cardiac delivery of therapeutic gelatin microspheres*. *Gene Ther*, 2006. **13**(18): p. 1320-7.
76. Wang, H., et al., *Injectable cardiac tissue engineering for the treatment of myocardial infarction*. *J Cell Mol Med*, 2010. **14**(5): p. 1044-55.
77. McFadden, D.G. and E.N. Olson, *Heart development: learning from mistakes*. *Curr Opin Genet Dev*, 2002. **12**(3): p. 328-35.
78. Kirby, M.L., *Cardiac development* 2007, Oxford ; New York: Oxford University Press. xiii, 273 p.
79. Linask, K.K., *N-cadherin localization in early heart development and polar expression of Na⁺,K⁺-ATPase, and integrin during pericardial coelom formation and epithelialization of the differentiating myocardium*. *Dev Biol*, 1992. **151**(1): p. 213-24.
80. Moreno-Rodriguez, R.A., et al., *Bidirectional fusion of the heart-forming fields in the developing chick embryo*. *Dev Dyn*, 2006. **235**(1): p. 191-202.
81. Abu-Issa, R. and M.L. Kirby, *Heart field: from mesoderm to heart tube*. *Annu Rev Cell Dev Biol*, 2007. **23**: p. 45-68.
82. Li, S., et al., *Advanced cardiac morphogenesis does not require heart tube fusion*. *Science*, 2004. **305**(5690): p. 1619-22.
83. Easton, H.S., R. Bellairs, and J.W. Lash, *Is chemotaxis a factor in the migration of precardiac mesoderm in the chick?* *Anat Embryol (Berl)*, 1990. **181**(5): p. 461-8.
84. Linask, K.K. and J.W. Lash, *Precardiac cell migration: fibronectin localization at mesoderm-endoderm interface during directional movement*. *Dev Biol*, 1986. **114**(1): p. 87-101.
85. George, E.L., H.S. Baldwin, and R.O. Hynes, *Fibronectins are essential for heart and blood vessel morphogenesis but are dispensable for initial specification of precursor cells*. *Blood*, 1997. **90**(8): p. 3073-81.
86. Trinh, L.A. and D.Y. Stainier, *Fibronectin regulates epithelial organization during myocardial migration in zebrafish*. *Dev Cell*, 2004. **6**(3): p. 371-82.
87. Buckingham, M., S. Meilhac, and S. Zaffran, *Building the mammalian heart from two sources of myocardial cells*. *Nat Rev Genet*, 2005. **6**(11): p. 826-35.
88. Dyer, L.A. and M.L. Kirby, *The role of secondary heart field in cardiac development*. *Dev Biol*, 2009. **336**(2): p. 137-44.
89. Zaffran, S. and R.G. Kelly, *New developments in the second heart field*. *Differentiation*, 2012. **84**(1): p. 17-24.

90. Waldo, K.L., et al., *Conotruncal myocardium arises from a secondary heart field*. Development, 2001. **128**(16): p. 3179-88.
91. Dyer, L.A. and M.L. Kirby, *Sonic hedgehog maintains proliferation in secondary heart field progenitors and is required for normal arterial pole formation*. Dev Biol, 2009. **330**(2): p. 305-17.
92. Sedmera, D., et al., *Developmental patterning of the myocardium*. Anat Rec, 2000. **258**(4): p. 319-37.
93. Icardo, J.M. and A. Fernandez-Teran, *Morphologic study of ventricular trabeculation in the embryonic chick heart*. Acta Anat (Basel), 1987. **130**(3): p. 264-74.
94. Liu, J., et al., *A dual role for ErbB2 signaling in cardiac trabeculation*. Development, 2010. **137**(22): p. 3867-75.
95. Wagner, M. and M.A. Siddiqui, *Signal transduction in early heart development (II): ventricular chamber specification, trabeculation, and heart valve formation*. Exp Biol Med (Maywood), 2007. **232**(7): p. 866-80.
96. Kuramochi, Y., X. Guo, and D.B. Sawyer, *Neuregulin activates erbB2-dependent src/FAK signaling and cytoskeletal remodeling in isolated adult rat cardiac myocytes*. J Mol Cell Cardiol, 2006. **41**(2): p. 228-35.
97. Nagy, II, et al., *Wnt-11 signalling controls ventricular myocardium development by patterning N-cadherin and beta-catenin expression*. Cardiovasc Res, 2010. **85**(1): p. 100-9.
98. Toyofuku, T., et al., *Guidance of myocardial patterning in cardiac development by *Sema6D* reverse signalling*. Nat Cell Biol, 2004. **6**(12): p. 1204-11.
99. van den Hoff, M.J. and A.F. Moorman, *Wnt, a driver of myocardialization?* Circ Res, 2005. **96**(3): p. 274-6.
100. Hoffman, J.I., *Incidence of congenital heart disease: II. Prenatal incidence*. Pediatr Cardiol, 1995. **16**(4): p. 155-65.
101. Hoffman, J.I., *Incidence of congenital heart disease: I. Postnatal incidence*. Pediatr Cardiol, 1995. **16**(3): p. 103-13.
102. Hoffman, J.I. and S. Kaplan, *The incidence of congenital heart disease*. J Am Coll Cardiol, 2002. **39**(12): p. 1890-900.
103. Lin, C.J., et al., *Partitioning the heart: mechanisms of cardiac septation and valve development*. Development, 2012. **139**(18): p. 3277-99.
104. Anderson, R.H., et al., *Development of the heart: (2) Septation of the atriums and ventricles*. Heart, 2003. **89**(8): p. 949-58.
105. Snarr, B.S., et al., *Isl1 expression at the venous pole identifies a novel role for the second heart field in cardiac development*. Circ Res, 2007. **101**(10): p. 971-4.
106. Briggs, L.E., J. Kakarla, and A. Wessels, *The pathogenesis of atrial and atrioventricular septal defects with special emphasis on the role of the dorsal mesenchymal protrusion*. Differentiation, 2012. **84**(1): p. 117-30.
107. Barlow, G.M., et al., *Down syndrome congenital heart disease: a narrowed region and a candidate gene*. Genet Med, 2001. **3**(2): p. 91-101.
108. Gittenberger-de Groot, A.C., et al., *Collagen type VI expression during cardiac development and in human fetuses with trisomy 21*. Anat Rec A Discov Mol Cell Evol Biol, 2003. **275**(2): p. 1109-16.

109. Grossman, T.R., et al., *Over-expression of DSCAM and COL6A2 cooperatively generates congenital heart defects*. PLoS Genet, 2011. **7**(11): p. e1002344.
110. Goddeeris, M.M., et al., *Intracardiac septation requires hedgehog-dependent cellular contributions from outside the heart*. Development, 2008. **135**(10): p. 1887-95.
111. van den Hoff, M.J., B.P. Kruithof, and A.F. Moorman, *Making more heart muscle*. Bioessays, 2004. **26**(3): p. 248-61.
112. Anderson, R.H., et al., *Development of the heart: (3) formation of the ventricular outflow tracts, arterial valves, and intrapericardial arterial trunks*. Heart, 2003. **89**(9): p. 1110-8.
113. Phillips, H.M., et al., *Vangl2 acts via RhoA signaling to regulate polarized cell movements during development of the proximal outflow tract*. Circ Res, 2005. **96**(3): p. 292-9.
114. Hakim, Z.S., et al., *Conditional deletion of focal adhesion kinase leads to defects in ventricular septation and outflow tract alignment*. Mol Cell Biol, 2007. **27**(15): p. 5352-64.
115. van den Hoff, M.J., et al., *Myocardialization of the cardiac outflow tract*. Dev Biol, 1999. **212**(2): p. 477-90.
116. Oishi, I., et al., *The receptor tyrosine kinase Ror2 is involved in non-canonical Wnt5a/JNK signalling pathway*. Genes Cells, 2003. **8**(7): p. 645-54.
117. Takeuchi, S., et al., *Mouse Ror2 receptor tyrosine kinase is required for the heart development and limb formation*. Genes Cells, 2000. **5**(1): p. 71-8.
118. Nomi, M., et al., *Loss of mRor1 enhances the heart and skeletal abnormalities in mRor2-deficient mice: redundant and pleiotropic functions of mRor1 and mRor2 receptor tyrosine kinases*. Mol Cell Biol, 2001. **21**(24): p. 8329-35.
119. Yu, H., et al., *Frizzled 1 and frizzled 2 genes function in palate, ventricular septum and neural tube closure: general implications for tissue fusion processes*. Development, 2010. **137**(21): p. 3707-17.
120. Gao, C. and Y.G. Chen, *Dishevelled: The hub of Wnt signaling*. Cell Signal, 2010. **22**(5): p. 717-27.
121. Matsumoto, S., et al., *Binding of APC and dishevelled mediates Wnt5a-regulated focal adhesion dynamics in migrating cells*. EMBO J, 2010. **29**(7): p. 1192-204.
122. Schleiffarth, J.R., et al., *Wnt5a is required for cardiac outflow tract septation in mice*. Pediatr Res, 2007. **61**(4): p. 386-91.
123. Zhou, W., et al., *Modulation of morphogenesis by noncanonical Wnt signaling requires ATF/CREB family-mediated transcriptional activation of TGFbeta2*. Nat Genet, 2007. **39**(10): p. 1225-34.
124. Cohen, E.D., et al., *Wnt5a and Wnt11 are essential for second heart field progenitor development*. Development, 2012. **139**(11): p. 1931-40.
125. Pankov, R. and K.M. Yamada, *Fibronectin at a glance*. J Cell Sci, 2002. **115**(Pt 20): p. 3861-3.
126. Leiss, M., et al., *The role of integrin binding sites in fibronectin matrix assembly in vivo*. Curr Opin Cell Biol, 2008. **20**(5): p. 502-7.
127. To, W.S. and K.S. Midwood, *Plasma and cellular fibronectin: distinct and independent functions during tissue repair*. Fibrogenesis Tissue Repair, 2011. **4**: p. 21.

128. Wierzbicka-Patynowski, I. and J.E. Schwarzbauer, *The ins and outs of fibronectin matrix assembly*. J Cell Sci, 2003. **116**(Pt 16): p. 3269-76.
129. Huttenlocher, A. and A.R. Horwitz, *Integrins in cell migration*. Cold Spring Harb Perspect Biol, 2011. **3**(9): p. a005074.
130. Vicente-Manzanares, M. and A.R. Horwitz, *Cell migration: an overview*. Methods Mol Biol, 2011. **769**: p. 1-24.
131. Wennerberg, K., et al., *Beta 1 integrin-dependent and -independent polymerization of fibronectin*. J Cell Biol, 1996. **132**(1-2): p. 227-38.
132. Wu, C., et al., *Integrin activation and cytoskeletal interaction are essential for the assembly of a fibronectin matrix*. Cell, 1995. **83**(5): p. 715-24.
133. Yang, J.T., H. Rayburn, and R.O. Hynes, *Embryonic mesodermal defects in alpha 5 integrin-deficient mice*. Development, 1993. **119**(4): p. 1093-105.
134. Danen, E.H., et al., *The fibronectin-binding integrins alpha5beta1 and alphavbeta3 differentially modulate RhoA-GTP loading, organization of cell matrix adhesions, and fibronectin fibrillogenesis*. J Cell Biol, 2002. **159**(6): p. 1071-86.
135. Truong, H. and E.H. Danen, *Integrin switching modulates adhesion dynamics and cell migration*. Cell Adh Migr, 2009. **3**(2): p. 179-81.
136. Knowlton, A.A., et al., *Rapid expression of fibronectin in the rabbit heart after myocardial infarction with and without reperfusion*. J Clin Invest, 1992. **89**(4): p. 1060-8.
137. Corda, S., J.L. Samuel, and L. Rappaport, *Extracellular matrix and growth factors during heart growth*. Heart Fail Rev, 2000. **5**(2): p. 119-30.
138. Dobaczewski, M., C. Gonzalez-Quesada, and N.G. Frangogiannis, *The extracellular matrix as a modulator of the inflammatory and reparative response following myocardial infarction*. J Mol Cell Cardiol, 2010. **48**(3): p. 504-11.
139. Daskalopoulos, E.P., B.J. Janssen, and W.M. Blankesteyn, *Myofibroblasts in the infarct area: concepts and challenges*. Microsc Microanal, 2012. **18**(1): p. 35-49.
140. Kohan, M., et al., *EDA-containing cellular fibronectin induces fibroblast differentiation through binding to alpha4beta7 integrin receptor and MAPK/Erk 1/2-dependent signaling*. FASEB J, 2010. **24**(11): p. 4503-12.
141. Port, F. and K. Basler, *Wnt trafficking: new insights into Wnt maturation, secretion and spreading*. Traffic, 2010. **11**(10): p. 1265-71.
142. Nishita, M., et al., *Cell/tissue-tropic functions of Wnt5a signaling in normal and cancer cells*. Trends Cell Biol, 2010. **20**(6): p. 346-54.
143. Komiya, Y. and R. Habas, *Wnt signal transduction pathways*. Organogenesis, 2008. **4**(2): p. 68-75.
144. Weeraratna, A.T., et al., *Wnt5a signaling directly affects cell motility and invasion of metastatic melanoma*. Cancer Cell, 2002. **1**(3): p. 279-88.
145. Dissanayake, S.K., et al., *The Wnt5A/protein kinase C pathway mediates motility in melanoma cells via the inhibition of metastasis suppressors and initiation of an epithelial to mesenchymal transition*. J Biol Chem, 2007. **282**(23): p. 17259-71.
146. Wang, Q., et al., *A novel role for Wnt/Ca2+ signaling in actin cytoskeleton remodeling and cell motility in prostate cancer*. PLoS ONE, 2010. **5**(5): p. e10456.
147. Yamamoto, H., et al., *Wnt5a signaling is involved in the aggressiveness of prostate cancer and expression of metalloproteinase*. Oncogene, 2010. **29**(14): p. 2036-46.

148. Gao, B., *Wnt regulation of planar cell polarity (PCP)*. Curr Top Dev Biol, 2012. **101**: p. 263-95.
149. Gao, B., et al., *Wnt signaling gradients establish planar cell polarity by inducing Vangl2 phosphorylation through Ror2*. Dev Cell, 2011. **20**(2): p. 163-76.
150. Schulte, G. and V. Bryja, *The Frizzled family of unconventional G-protein-coupled receptors*. Trends Pharmacol Sci, 2007. **28**(10): p. 518-25.
151. Slusarski, D.C., V.G. Corces, and R.T. Moon, *Interaction of Wnt and a Frizzled homologue triggers G-protein-linked phosphatidylinositol signalling*. Nature, 1997. **390**(6658): p. 410-3.
152. Slusarski, D.C., et al., *Modulation of embryonic intracellular Ca²⁺ signaling by Wnt-5A*. Dev Biol, 1997. **182**(1): p. 114-20.
153. Kikuchi, A., et al., *Wnt5a: its signalling, functions and implication in diseases*. Acta Physiol (Oxf), 2012. **204**(1): p. 17-33.
154. He, F., et al., *Wnt5a regulates directional cell migration and cell proliferation via Ror2-mediated noncanonical pathway in mammalian palate development*. Development, 2008. **135**(23): p. 3871-9.
155. Nomachi, A., et al., *Receptor tyrosine kinase Ror2 mediates Wnt5a-induced polarized cell migration by activating c-Jun N-terminal kinase via actin-binding protein filamin A*. J Biol Chem, 2008. **283**(41): p. 27973-81.
156. Witze, E.S., et al., *Wnt5a control of cell polarity and directional movement by polarized redistribution of adhesion receptors*. Science, 2008. **320**(5874): p. 365-9.
157. Liu, Y., et al., *Wnt5a induces homodimerization and activation of Ror2 receptor tyrosine kinase*. J Cell Biochem, 2008. **105**(2): p. 497-502.
158. Liu, Y., et al., *Homodimerization of Ror2 tyrosine kinase receptor induces 14-3-3(beta) phosphorylation and promotes osteoblast differentiation and bone formation*. Mol Endocrinol, 2007. **21**(12): p. 3050-61.
159. Bergmann, M.W., *WNT signaling in adult cardiac hypertrophy and remodeling: lessons learned from cardiac development*. Circ Res, 2010. **107**(10): p. 1198-208.
160. He, W., et al., *Exogenously administered secreted frizzled related protein 2 (Sfrp2) reduces fibrosis and improves cardiac function in a rat model of myocardial infarction*. Proc Natl Acad Sci U S A, 2010. **107**(49): p. 21110-5.
161. Mirotsov, M., et al., *Secreted frizzled related protein 2 (Sfrp2) is the key Akt-mesenchymal stem cell-released paracrine factor mediating myocardial survival and repair*. Proc Natl Acad Sci U S A, 2007. **104**(5): p. 1643-8.
162. Laeremans, H., et al., *Wnt/frizzled signalling modulates the migration and differentiation of immortalized cardiac fibroblasts*. Cardiovasc Res, 2010. **87**(3): p. 514-23.
163. Minami, Y., et al., *Ror-family receptor tyrosine kinases in noncanonical Wnt signaling: their implications in developmental morphogenesis and human diseases*. Dev Dyn, 2010. **239**(1): p. 1-15.
164. Toyofuku, T., et al., *Wnt/frizzled-2 signaling induces aggregation and adhesion among cardiac myocytes by increased cadherin-beta-catenin complex*. J Cell Biol, 2000. **150**(1): p. 225-41.

165. van Gijn, M.E., et al., *Frizzled 2 is transiently expressed in neural crest-containing areas during development of the heart and great arteries in the mouse*. *Anat Embryol (Berl)*, 2001. **203**(3): p. 185-92.
166. Etheridge, S.L., et al., *Murine dishevelled 3 functions in redundant pathways with dishevelled 1 and 2 in normal cardiac outflow tract, cochlea, and neural tube development*. *PLoS Genet*, 2008. **4**(11): p. e1000259.
167. Henderson, D.J., et al., *Cardiovascular defects associated with abnormalities in midline development in the Loop-tail mouse mutant*. *Circ Res*, 2001. **89**(1): p. 6-12.
168. Corti, S., et al., *Chemotactic factors enhance myogenic cell migration across an endothelial monolayer*. *Exp Cell Res*, 2001. **268**(1): p. 36-44.
169. Zakharova, L., et al., *Transplantation of cardiac progenitor cell sheet onto infarcted heart promotes cardiogenesis and improves function*. *Cardiovasc Res*, 2010. **87**(1): p. 40-9.
170. Bock-Marquette, I., et al., *Thymosin beta4 activates integrin-linked kinase and promotes cardiac cell migration, survival and cardiac repair*. *Nature*, 2004. **432**(7016): p. 466-72.
171. Shiba, Y., et al., *Human ES-cell-derived cardiomyocytes electrically couple and suppress arrhythmias in injured hearts*. *Nature*, 2012.
172. Bartram, U., et al., *Double-outlet right ventricle and overriding tricuspid valve reflect disturbances of looping, myocardialization, endocardial cushion differentiation, and apoptosis in TGF-beta(2)-knockout mice*. *Circulation*, 2001. **103**(22): p. 2745-52.
173. Bouchev, D., W.S. Argraves, and C.D. Little, *Fibulin-1, vitronectin, and fibronectin expression during avian cardiac valve and septa development*. *Anat Rec*, 1996. **244**(4): p. 540-51.
174. Hilenski, L.L., L. Terracio, and T.K. Borg, *Myofibrillar and cytoskeletal assembly in neonatal rat cardiac myocytes cultured on laminin and collagen*. *Cell Tissue Res*, 1991. **264**(3): p. 577-87.
175. Klewer, S.E., et al., *Expression of type VI collagen in the developing mouse heart*. *Dev Dyn*, 1998. **211**(3): p. 248-55.
176. Hutson, M.R., et al., *Cardiac arterial pole alignment is sensitive to FGF8 signaling in the pharynx*. *Dev Biol*, 2006. **295**(2): p. 486-97.
177. Chen, W., et al., *Dishevelled 2 recruits beta-arrestin 2 to mediate Wnt5A-stimulated endocytosis of Frizzled 4*. *Science*, 2003. **301**(5638): p. 1391-4.
178. Xu, C., et al., *Efficient generation and cryopreservation of cardiomyocytes derived from human embryonic stem cells*. *Regen Med*, 2011. **6**(1): p. 53-66.
179. Zhu, W.Z., et al., *Neuregulin/ErbB signaling regulates cardiac subtype specification in differentiating human embryonic stem cells*. *Circ Res*, 2010. **107**(6): p. 776-86.
180. Salva, M.Z., et al., *Design of tissue-specific regulatory cassettes for high-level rAAV-mediated expression in skeletal and cardiac muscle*. *Mol Ther*, 2007. **15**(2): p. 320-9.
181. Mai, J., et al., *Axon initiation and growth cone turning on bound protein gradients*. *J Neurosci*, 2009. **29**(23): p. 7450-8.
182. Zantl, R. and E. Horn, *Chemotaxis of slow migrating mammalian cells analysed by video microscopy*. *Methods Mol Biol*, 2011. **769**: p. 191-203.
183. Zigmond, S.H., *Ability of polymorphonuclear leukocytes to orient in gradients of chemotactic factors*. *J Cell Biol*, 1977. **75**(2 Pt 1): p. 606-16.

184. Olivares-Navarrete, R., et al., *Role of non-canonical Wnt signaling in osteoblast maturation on microstructured titanium surfaces*. Acta Biomater, 2011. **7**(6): p. 2740-50.
185. Vuga, L.J., et al., *WNT5A is a regulator of fibroblast proliferation and resistance to apoptosis*. Am J Respir Cell Mol Biol, 2009. **41**(5): p. 583-9.
186. Yamamoto, H., et al., *Wnt5a signaling is involved in the aggressiveness of prostate cancer and expression of metalloproteinase*. Oncogene, 2010. **29**(14): p. 2036-46.
187. Laeremans, H., et al., *Blocking of frizzled signaling with a homologous peptide fragment of wnt3a/wnt5a reduces infarct expansion and prevents the development of heart failure after myocardial infarction*. Circulation, 2011. **124**(15): p. 1626-35.
188. Takeuchi, J.K., et al., *Chromatin remodelling complex dosage modulates transcription factor function in heart development*. Nat Commun, 2011. **2**: p. 187.
189. Mandeville, J.T., R.N. Ghosh, and F.R. Maxfield, *Intracellular calcium levels correlate with speed and persistent forward motion in migrating neutrophils*. Biophys J, 1995. **68**(4): p. 1207-17.
190. Rhoads, D.S. and J.L. Guan, *Analysis of directional cell migration on defined FN gradients: role of intracellular signaling molecules*. Exp Cell Res, 2007. **313**(18): p. 3859-67.
191. Ahuja, P., et al., *Sequential myofibrillar breakdown accompanies mitotic division of mammalian cardiomyocytes*. J Cell Sci, 2004. **117**(Pt 15): p. 3295-306.
192. van Laake, L.W., et al., *Extracellular matrix formation after transplantation of human embryonic stem cell-derived cardiomyocytes*. Cell Mol Life Sci, 2010. **67**(2): p. 277-90.
193. Howlett, A., *Integrin protocols*. Methods in molecular biology 1999, Totowa, N.J.: Humana Press. xi, 296 p.
194. Okoye, U.C., C.C. Malbon, and H.Y. Wang, *Wnt and Frizzled RNA expression in human mesenchymal and embryonic (H7) stem cells*. J Mol Signal, 2008. **3**: p. 16.
195. Davies, G.E., et al., *Genetic-Variation in the Col6a1 Region Is Associated with Congenital Heart-Defects in Trisomy-21 (Downs-Syndrome)*. Annals of Human Genetics, 1995. **59**: p. 253-269.
196. Davies, G.E., et al., *Unusual genotypes in the COL6A1 gene in parents of children with trisomy 21 and major congenital heart defects*. Hum Genet, 1994. **93**(4): p. 443-6.
197. Delom, F., et al., *Transchromosomal cell model of Down syndrome shows aberrant migration, adhesion and proteome response to extracellular matrix*. Proteome Sci, 2009. **7**: p. 31.
198. Sinha, T., et al., *Disheveled mediated planar cell polarity signaling is required in the second heart field lineage for outflow tract morphogenesis*. Dev Biol, 2012. **370**(1): p. 135-44.
199. Lim, J.J., et al., *Development of nano- and microscale chondroitin sulfate particles for controlled growth factor delivery*. Acta Biomater, 2011. **7**(3): p. 986-95.
200. Kinney, M.A. and T.C. McDevitt, *Emerging strategies for spatiotemporal control of stem cell fate and morphogenesis*. Trends Biotechnol, 2013. **31**(2): p. 78-84.
201. Ghosh, K., et al., *Fibronectin functional domains coupled to hyaluronan stimulate adult human dermal fibroblast responses critical for wound healing*. Tissue Eng, 2006. **12**(3): p. 601-13.

202. Seidlits, S.K., et al., *Fibronectin-hyaluronic acid composite hydrogels for three-dimensional endothelial cell culture*. Acta Biomater, 2011. **7**(6): p. 2401-9.
203. Naugle, J.E., et al., *Type VI collagen induces cardiac myofibroblast differentiation: implications for postinfarction remodeling*. Am J Physiol Heart Circ Physiol, 2006. **290**(1): p. H323-30.
204. Bujak, M. and N.G. Frangogiannis, *The role of TGF-beta signaling in myocardial infarction and cardiac remodeling*. Cardiovasc Res, 2007. **74**(2): p. 184-95.
205. Chen, H., et al., *Gene expression changes associated with fibronectin-induced cardiac myocyte hypertrophy*. Physiol Genomics, 2004. **18**(3): p. 273-83.
206. Kruithof, B.P., et al., *Cardiac muscle cell formation after development of the linear heart tube*. Dev Dyn, 2003. **227**(1): p. 1-13.
207. Kurayoshi, M., et al., *Expression of Wnt-5a is correlated with aggressiveness of gastric cancer by stimulating cell migration and invasion*. Cancer Res, 2006. **66**(21): p. 10439-48.
208. Tomar, A. and D.D. Schlaepfer, *Focal adhesion kinase: switching between GAPs and GEFs in the regulation of cell motility*. Curr Opin Cell Biol, 2009. **21**(5): p. 676-83.
209. Cao, J., et al., *Membrane type 1 matrix metalloproteinase induces epithelial-to-mesenchymal transition in prostate cancer*. J Biol Chem, 2008. **283**(10): p. 6232-40.
210. Kamino, M., et al., *Wnt-5a signaling is correlated with infiltrative activity in human glioma by inducing cellular migration and MMP-2*. Cancer Sci, 2011. **102**(3): p. 540-8.